Soft Matter

CrossMark
click for updates

Effects of molecular chirality on self-assembly and switching in liquid crystals at the cross-over between rod-like and bent shapes†

Hale Ocak,*[ab] Marco Poppe,[a] Belkız Bilgin-Eran,[b] Gürkan Karanlık,[b] Marko Prehm[a] and Carsten Tschierske*[a]

A bent-core compound derived from a 4-cyanoresorcinol core unit with two terephthalate based rod-like wings and carrying chiral 3,7-dimethyloctyloxy side chains has been synthesized in racemic and enantiomerically pure form and characterized by polarizing microscopy, differential scanning calorimetry, X-ray diffraction and electro-optical investigations to study the influence of molecular chirality on the superstructural chirality and polar order in lamellar liquid crystalline phases. Herein we demonstrate that the coupling of molecular chirality with superstructural layer chirality in SmC_sP_F domain phases (forming energetically distinct diastereomeric pairs) can fix the tilt direction and thus stabilize synpolar order, leading to bistable ferroelectric switching in the SmC* phases of the (S)-enantiomer, whereas tristable modes determine the switching of the racemate. Moreover, the mechanism of electric field induced molecular reorganization changes from a rotation around the molecular long axis in the racemate to a rotation on the tilt-cone for the (S)-enantiomer. At high temperature the enantiomer behaves like a rod-like molecule with a chirality induced ferroelectric SmC* phase and an electroclinic effect in the SmA'* phase. At reduced temperature sterically induced polarization, due to the bent molecular shape, becomes dominating, leading to much higher polarization values, thus providing access to high polarization ferroelectric materials with weakly bent compounds having only "weakly chiral" stereogenic units. Moreover, the field induced alignment of the $SmC_sP_F^{(*)}$ domains gives rise to a special kind of electroclinic effect appearing even in the absence of molecular chirality. Comparison with related compounds indicates that the strongest effects of chirality appear for weakly bent molecules with a relatively short coherence length of polar order, whereas for smectic phases with long range polar order the effects of the interlayer interfaces can override the chirality effects.

1. Introduction

Ferroelectricity, *i.e.* the spontaneous formation of macroscopic polar order, capable of being switched between two polar states, represents an important field of materials science. In particular, organic ferroelectrics have aroused recent interest as an emerging field.[1] A special attractive feature of these organic materials is the access to soft ferroelectrics with numerous new applications which are not possible with related solid state materials.[2]

There are presently two distinct types of soft ferroelectrics, representing smectic liquid crystals (LCs).[3] One type is formed by chiral molecules organized in layers and assuming a uniform tilt (SmC* phases).[4] The other one is provided by so-called bent-core molecules which are also organized in layers.[5–8] For these molecules the bent shape restricts the rotation around the long axis, thus producing sterically induced polar order ($SmCP_F$ and $SmAP_F$ phases) due to the directed packing of the bent molecules with a uniform bending direction.[9,10] In this case neither chirality nor tilt is required for the occurrence of polar order and ferroelectricity. For the tilted LC phases of bent-core liquid crystals (BCLCs) there are four distinct structures depending on the tilt direction and the polar direction, designated as SmC_sP_F, SmC_sP_A, SmC_aP_F and SmC_aP_A and shown in Fig. 1a.[11]

An interesting question concerns the combination of the two distinct approaches to ferroelectricity by introducing a bend into chiral rod-like mesogens or by introducing chirality into bent-core mesogens by molecular design,[12–14] or by mixing achiral bent-core mesogens with rod-like chiral compounds.[13]

[a] *Institute of Chemistry, Organic Chemistry, Martin Luther University Halle-Wittenberg, Kurt-Mothes-Str. 2, D-06120 Halle, Germany. E-mail: ocak_hale@hotmail.com, carsten.tschierske@chemie.uni-halle.de*

[b] *Department of Chemistry, Yildiz Technical University, Davutpasa Yerlesim Birimi, TR-34220 Esenler, Istanbul, Turkey*

† Electronic supplementary information (ESI) available. See DOI: 10.1039/c6sm00960c
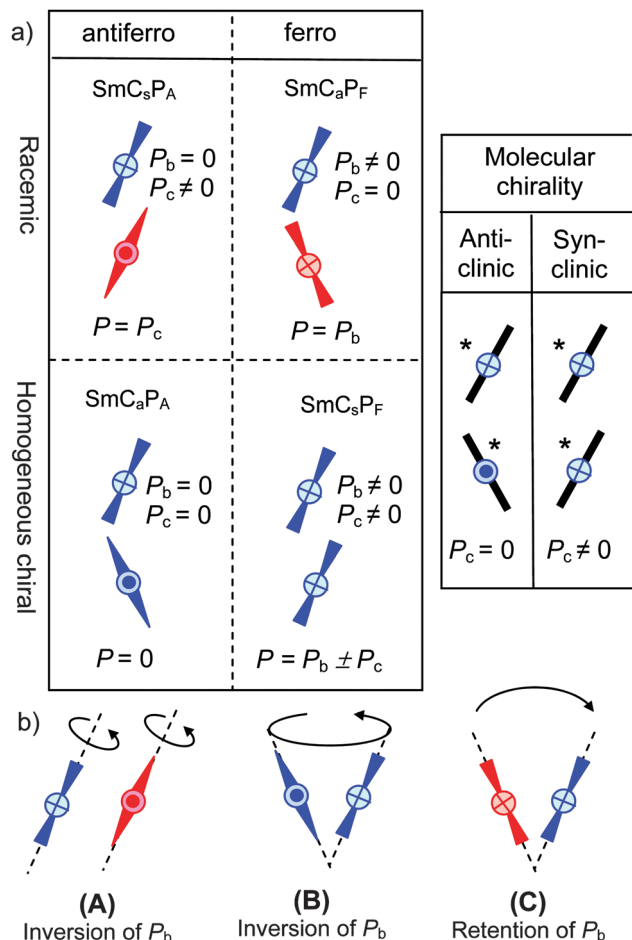
a)

	antiferro	ferro

Racemic — SmC_sP_A — $P_b = 0$, $P_c \neq 0$ — $P = P_c$; SmC_aP_F — $P_b \neq 0$, $P_c = 0$ — $P = P_b$

Homogeneous chiral — SmC_aP_A — $P_b = 0$, $P_c = 0$ — $P = 0$; SmC_sP_F — $P_b \neq 0$, $P_c \neq 0$ — $P = P_b \pm P_c$

Molecular chirality

Anti-clinic	Syn-clinic
*	*
*	*
$P_c = 0$	$P_c \neq 0$

b)

(A) Inversion of P_b (B) Inversion of P_b (C) Retention of P_b

Fig. 1 (a) The four states of the SmCP phases of bent core molecules[11] and the contribution of core packing (P_b) and a combination of molecular chirality and the tilt-direction (P_c, right) to the overall polarization P;[15] the molecules are shown in a side view along the polar axis and the color indicates the sign of the superstructural layer chirality; (b) the effect of the distinct switching and reorganization modes of chiral BCLCs on P_b (P_c is fixed by the molecular chirality) and superstructural layer chirality; (**A**) rotation around the long axis; (**B**) rotation on the tilt cone and (**C**) flipping of the tilt direction.[29]

and uniformly chiral structures (SmC_sP_F and SmC_aP_A) with identical layer chirality which can exist in two enantiomeric forms (blue or red, only one enantiomer of the chiral structures is shown in Fig. 1a).[11] In line with the basic concepts of stereochemistry it was shown that in the chiral synclinic ferro-electric phases or states (SmC_sP_F*) the sign of the tilt is coupled with the molecular chirality, as only one combination of molecular and superstructural chirality represents the low energy diastereomer (matched case) and the other diastereomer is disfavored (mismatched case).[15] However, surprisingly it was also observed that enantiomerically enriched chiral bent-core molecules preferably form synclinic antiferroelectric (SmC_sP_A*) and anticlinic ferroelectric (SmC_aP_F*) structures, which represent racemic structures with alternating right and left handed layers (Fig. 1a).[16] This was explained by a dominance of the effects of interlayer interfaces[9,17] on tilt correlation over the effects of molecular chirality. However, these investigations were based on the comparison of homogeneously chiral molecules, involving branched alkyl chains with achiral molecules comprising linear n-alkyl chains, representing different molecular structures.[18–27] As there are significant effects of chain branching on interlayer coupling, mesophase type and mode of switching,[9,16,20,22,23] this investigation cannot be fully conclusive and direct comparisons of uniformly chiral compounds with their racemic mixtures would be required. There is only a handful of reports about this kind of comparison[28–31] and some of them have only appeared in conference proceedings[15] or were only partly published.[32] Moreover, previous work in this field was mostly focused on strongly bent molecules (with about 120° angles),[16,19,21,23,26,28] forming the typical macroscopic polar "banana" phases composed of polar layers (see Fig. 1a). However, there are also bent-core molecules with reduced bend which, depending on temperature, can change their shape from nearly rod-like to strongly bent and therefore show transitions between non-polar LC phases and polar "banana" phases.[33–37] Typical compounds are provided by benzoylated 4-cyanoresorcinols,[36–42] having a reduced molecular bend due to the effect of the 4-CN substituent on the conformation of the adjacent COO linking unit.[38]

An especially interesting case is provided by compound **1**.[29] In the SmC_sP_A* phase of the enantiomer (S)-**1** (see Fig. 2a) the switching of the field induced SmC_sP_F* state by rotation around the long axis (process (**A**) in Fig. 1b) inverts the sign of the layer chirality, whereas the molecular chirality cannot change; this leads to a diastereomeric state which after switching no longer represents the energetic minimum (mismatched case). Under the applied field the energetically preferred diastereomeric state (matched case) is re-established in a relaxation process by tilt-flipping without inversion of the polar direction (see (C) in Fig. 1b and 2b).[29]

Here we report a new bent-core molecule **2** based on the same 4-cyanoresorcinol core, but with terephthalate based rod-like wings,[43–45] replacing the biphenyls in compound **1**, and carrying the same chiral 3,7-dimethyloctyloxy groups[46] in the racemic (*rac*-**2**) and the uniformly chiral (S,S)-form ((S)-**2**, see Table 1). Just like compound **1**, compound **2** shows a non-polar SmA phase and tilted smectic phases (SmC), but these SmC
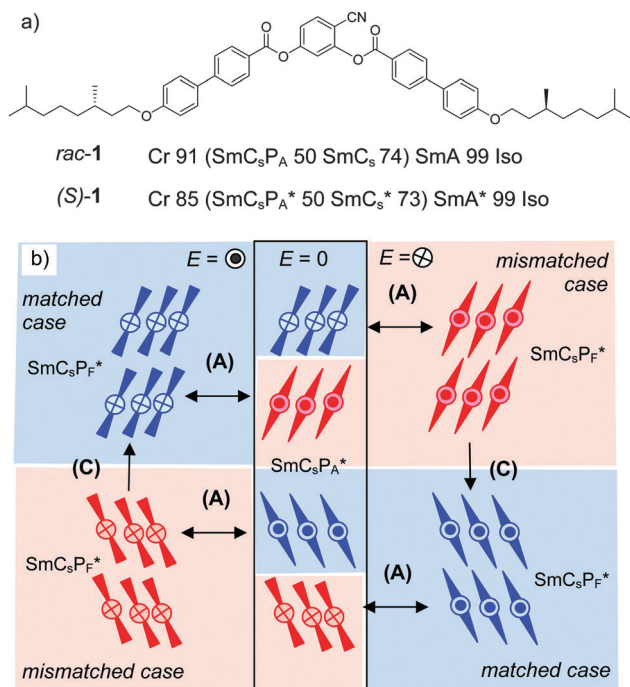
For these combined systems the coexistence of two kinds of polarization, one due to the packing of the bent-cores (bent-core polarization: P_b) and the other one resulting from molecular chirality, leading to reduced local symmetry (C_2) and coupling with the tilt direction, as known in SmC* phases (chirality polarization: P_c), is in principle possible (see Fig. 1a).[15]

Besides the molecular chirality, chirality at the superstructural level must also be considered in the polar SmC phases of bent-core mesogens. As the combination of tilt and polar order gives rise to a reduced C_2 symmetry, these layers are inherently chiral and their chirality is reversed either by tilt reversal or by reversal of the polar direction, whereas simultaneously reversing both tilt and polar directions, retains the chirality (Fig. 1b).[11] Depending on the mode of combination of the polar direction and the tilt direction in adjacent layers the four different phase structures can be divided into racemic structures with alternating chirality (red + blue) in adjacent layers (SmC_sP_A and SmC_aP_F)

a)

rac-1	Cr 91 (SmC$_s$P$_A$ 50 SmC$_s$ 74) SmA 99 Iso
(S)-1	Cr 85 (SmC$_s$P$_A$* 50 SmC$_s$* 73) SmA* 99 Iso

Fig. 2 (a) Chemical structure, LC phases and transition temperatures (T/°C) of the pure enantiomer and the racemic mixture of compound 1;[29] values in parenthesis are monotropic phases which can only be observed on cooling; abbreviations: Cr = crystalline solid state; Iso = isotropic liquid state; SmA = non-tilted and nonpolar smectic phase; SmC$_s$ = non-polar and synclinic tilted smectic phase; SmC$_s$P$_A$ = synclinic tilted and antiferroelectric switching polar SmC phase (see Fig. 1a); the asterisk (*) indicates LC phases formed by uniform chiral molecules, being affected by the molecular chirality (favoring the layer chirality indicated in blue); (b) molecular reorganization during the antiferroelectric switching by rotation around the long axis (A) and relaxation to the thermodynamically more stable (matched) state by tilt flipping (C) under the applied field (see Fig. 1b), as observed for (S)-1.[29]

phases are very distinct from those of the related compound 1 where only one type of antiferroelectric switching SmC$_s$P$_A$$^{(*)}$

phase was observed for the racemate and the enantiomer. In contrast, for compound 2 a sequence of paraelectric and superparaelectric SmC phase ranges is found for the racemate which is replaced by SmC* phases showing distinct ferroelectric modes for the enantiomer. This shows that coupling of molecular chirality with the superstructural layer chirality in SmC$_s$P$_F$* domains stabilizes synpolar correlation which provides access to high polarization ferroelectric materials with weakly bent compounds having only "weakly chiral" stereogenic units. In addition, classical and non-classical electroclinic effects[4] were found for enantiomers and racemates which are associated with the field induced alignment of the local domain structure of the smectic phases of 2. Conclusions are drawn concerning the interplay between chirality induced and sterically induced polar order.

2. Results and discussion

2.1 Synthesis

The 4-cyanoresorcinol based bent-core molecules (S)-2 and rac-2 were synthesized as shown in Scheme 1 from 2,4-dihydroxybenzonitrile[38] (A) and benzoic acid B. A was synthesized from commercially available 2,4-dihydroxybenzaldehyde by the formation of the oxime, followed by dehydration as described previously.[36] For the synthesis of 4-[4-(3,7-dimethyloctyloxy)phenoxycarbonyl]benzoic acid (S)-B, (S)-(−)-β-citronellol was firstly reduced to give (S)-3,7-dimethyl-1-octanol under catalytic hydrogenation conditions (H$_2$, Pd/C in MeOH) and then brominated to give (S)-3,7-dimethyloctyl-1-bromide.[47] Etherification with 4-benzyloxyphenol, followed by hydrogenolytic debenzylation, yields (S)-4-(3,7-dimethyloctyloxy)phenol.[48] The esterification reaction of this phenol with 4-formylbenzoic acid using DCC and DMAP, followed by oxidation using sodium chlorite as an oxidizing agent leads to benzoic acid (S)-B. The racemic benzoic acid B (rac-B) was also prepared in a similar way from racemic 3,7-dimethyl-1-octanol

Table 1 Mesophases and phase transition temperatures of the compound (S)-2 and the racemic mixure rac-2^a

Compd	T/°C [ΔH kJ mol^{-1}]
rac-2	Cr 98 [33.8]^b (SmC$_a$'P$_A$ 73 [—] SmC$_s$'P$_A$ 81 [2.4] SmCP$_{AR}$ 87 [—] SmC 93 [—]) SmA' 105 [—] SmA 159 [6.8] Iso
(S)-2	Cr 106 [46.0]^b (SmC$_a$'P$_A$* 73 [—] SmC$_s$'P$_F$* 81 [2.2] SmCP$_R$* 87 [—] SmC* 93 [—] SmA'* 105 [—]) SmA* 159 [6.8] Iso

^{a} Transition temperatures as determined by the polarizing microscope under quasi equilibrium conditions and enthalpy values in italics in brackets taken from the 1st heating and cooling scans at a rate of 10 K min^{-1}, see the Experimental section; abbreviations: SmA = uniaxial smectic phase, the prime in SmA' indicates a de Vries-like SmC phase composed of tilt randomized SmC domains; SmC = paraelectric SmC phase; SmCP$_R$*, SmCP$_{AR}$ = tilted smectic phases composed of SmC$_s$P$_F$ domains (in the domains the tilt direction and the polar direction are uniform), with preferred synpolar (SmCP$_R$*) or antipolar (SmCP$_{AR}$) Ising-like correlation of the domains;[57] SmC$_s$'P$_F$* = ferroelectric switching polar smectic phase with a uniform (synclinic) tilt; SmC$_s$'P$_A$ = high permittivity paraelectric smectic phase with a synclinic tilt; SmC$_a$'P$_A$ = high permittivity paraelectric smectic phase with an anticlinic tilt; SmC$_a$'P$_A$* = ferroelectric switching polar smectic phase with slow relaxation to a SmC$_a$'P$_A$ ground state structure; the prime in the phase designation indicates a special domain-like structure of these polar smectic phases which are distinct from the typical B$_2$ phases; for other abbreviations, see Fig. 2. ^{b} Melting point of the highest temperature crystalline phase is given and the enthalpy value is the sum of all Cr–Cr transitions and melting events (see Fig. 3).
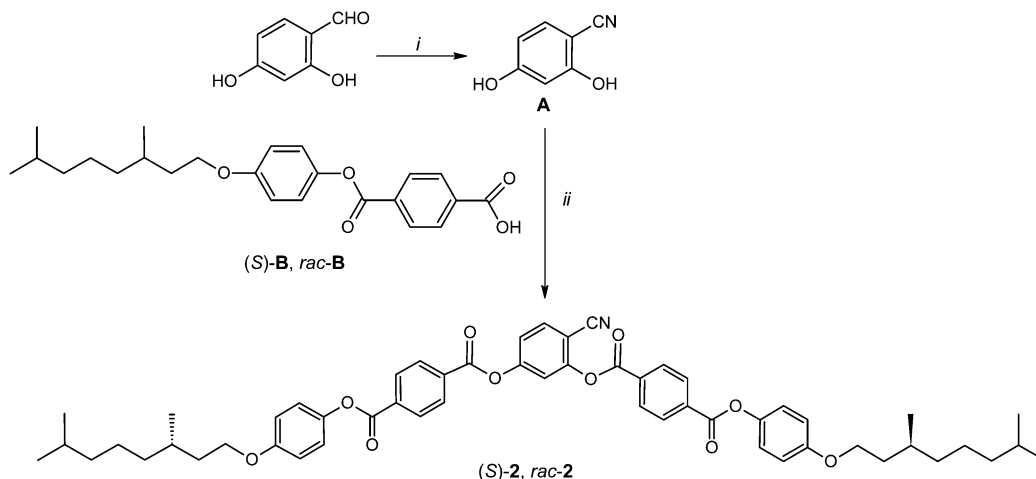
Scheme 1 Synthesis of the bent-core compound (S)-**2** and its racemic mixture rac-**2**. Reagents and conditions: (i) (1) NH$_2$OH·HCl, (2) Ac$_2$O, (3) KOH;[38] (ii) DCC, DMAP, CH$_2$Cl$_2$.

via the tosylate as described previously.[49] (S)-**2** and rac-**2** were obtained by esterification of 2,4-dihydroxybenzonitrile (**A**) with rac-**B** and (S)-**B**, using dicyclohexylcarbodiimide (DCC) and 4-dimethylaminopyridine (DMAP) as a catalyst[50] in dry dichloromethane. The experimental details, spectroscopic (^{1}H- and ^{13}C-NMR) data and elemental analysis data for the compounds are given in the ESI.†

Throughout all steps of the synthesis of the enantiomer (S)-**2** the stereogenic center of the (S)-3,7-dimethyloctyloxy group was not touched and hence it can be assumed that the final product has approximately equal optical purity as (S)-(−)-β-citronellol (≥99%), used as a starting material.[29,31,51] rac-**2** represents an optically inactive racemic mixture of the (R,R), (S,S), (R,S) and (S,R) stereoisomers. Despite being a complex mixture, the LC phase transition temperatures and the sharpness of the phase transitions are the same as for the enantiomeric pure single component compound (S)-**2** (see Fig. 3).

2.2 Liquid crystalline ground state structures

The observed transition temperatures, corresponding enthalpy values and mesophase types of (S)-**2** and rac-**2** are summarized in Table 1, and Fig. 3 shows the DSC heating and cooling traces. Both, (S)-**2** and rac-**2**, show multiple crystalline modifications with the most stable crystal modification melting at $T = 98\ ^\circ$C for the racemate and at $T = 106\ ^\circ$C for (S)-**2**. On cooling no crystallization is observed down to room temperature.

In the cooling scans there are two exotherms for (S)-**2** and rac-**2**, occurring at almost the same temperature, a larger one ($\Delta H = -6.7$ kJ mol^{-1}) for the iso–LC transition at $T = 159\ ^\circ$C and a smaller one ($\Delta H \sim -2.8$ kJ mol^{-1}) for an additional phase transition in the LC range at $T = 81\ ^\circ$C. Besides these phase transitions with enthalpy changes, there are four additional continuous transitions in the LC range without visible enthalpy change, occurring at $T = 105, 93, 87$ and $73\ ^\circ$C. So, in total, six distinct LC ranges can be distinguished. The high temperature phase (SmA$^{(*)}$, for rac-**2** also a certain range of SmA′) is enantiotropic, whereas the tilted LC phases (SmC$^{(*)}$ and the
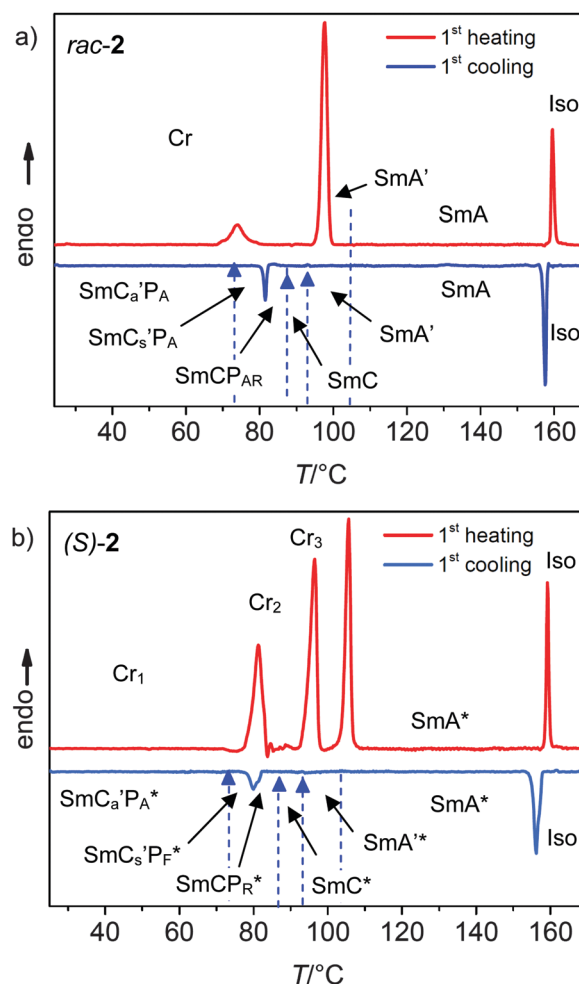

Fig. 3 DSC heating and cooling traces (10 K min^{-1}) of (a) rac-**2** and (b) (S)-**2**.

randomly tilted SmA′* phases) are monotropic (metastable) and therefore could only be observed on cooling from the SmA$^{(*)}$ phase. Nevertheless, the monotropic phases are long

time persistent and thus can be investigated by different methods. In the following sections the discussion is focused on the four smectic phases above $T = 73\ °C$, whereas the low temperature phase ($SmC_a'P_A^{(*)}$) below this temperature will be discussed separately in Section 2.3.4.

2.2.1 LC phases of *rac*-2. On cooling the racemic mixture *rac*-2 to $T = 159\ °C$ the first order phase transition from the isotropic liquid leads to a typical fan-shaped texture in planar samples (Fig. 4a) and a pseudoisotropic appearance under homeotropic anchoring (inset in Fig. 4a), as typical for a non-tilted smectic (SmA) phase. On further cooling *rac*-2 in a planar cell (layers perpendicular to the substrates) the birefringence color changes from red to purple/blue indicating a growing birefringence with decreasing temperature (Fig. 4a and b). The fans break at 93 °C (Fig. 4b, see also Fig. S5b and c, ESI†), but there is no observable DSC peak at this continuous transition. At the transition at $T = 81\ °C$, which is associated with a DSC peak, the birefringence further increases (pink/blue to green, see Fig. 4c). In homeotropic

samples of *rac*-2 (layers parallel to the substrates) the optically uniaxial SmA phase appears completely dark (pseudo-isotropic) and the formation of a birefringent Schlieren texture is observed at $T = 93\ °C$ (see the inset in Fig. 4b), indicating the transition to an optically biaxial LC phase. The Schlieren texture continuously increases in birefringence on further cooling with a clearly visible textural change and an increase of birefringence at the transition at $T = 81\ °C$ (inset in Fig. 4c).

XRD investigations of surface aligned samples of *rac*-2 at $T = 130\ °C$ in the SmA phase indicate a sharp small angle reflection at $d = 4.34$ nm with the corresponding second order reflection having the maximum positioned on the meridian and a diffuse wide angle scattering ($d = 0.48$ nm) having its maxima on the equator, in line with the proposed SmA structure (Fig. 5a). The observed d-value is only a bit smaller than the molecular length ($L_{mol} = 5.0$ nm; $d/L_{mol} = 0.86–0.87$), thus indicating a monolayer smectic phase, allowing a possible maximum tilt angle of 30°.

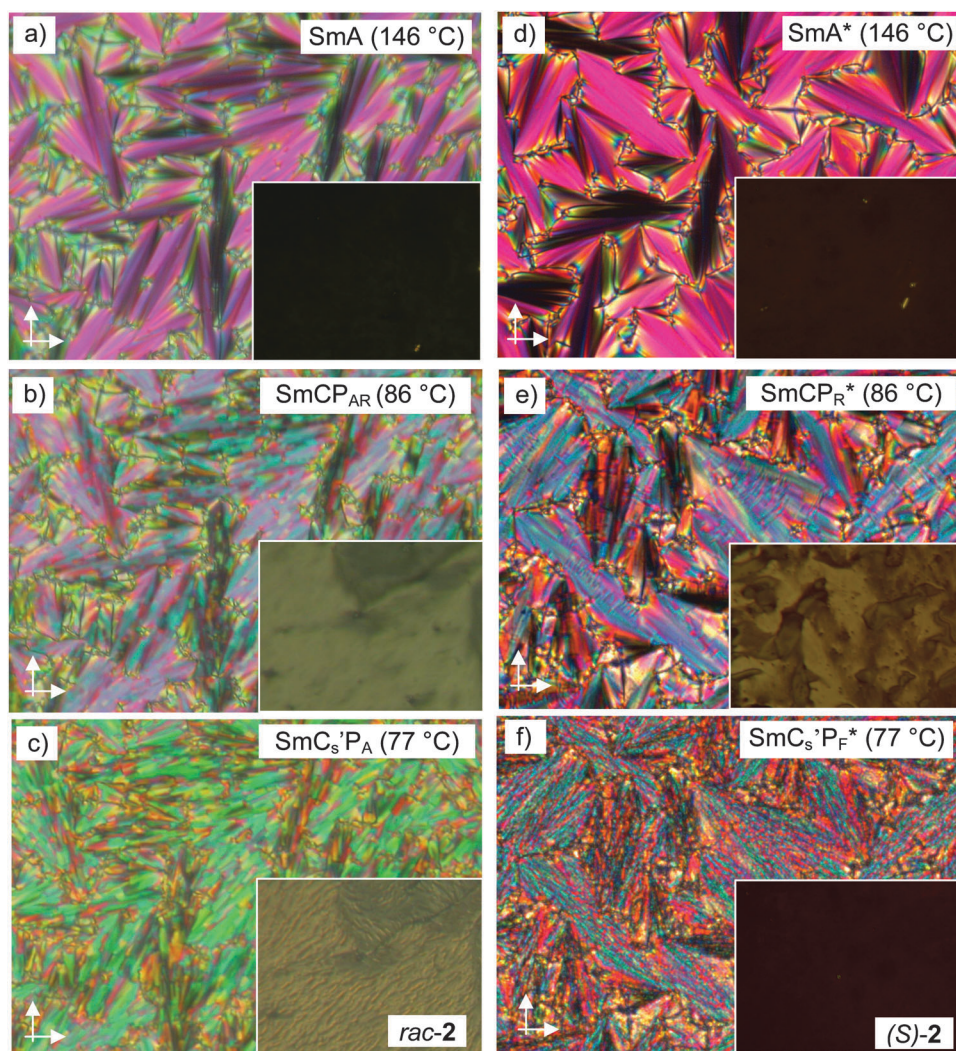**Fig. 4** Textures of the LC phases of (a–c) *rac*-2 (left) and (d–f) (*S*)-2 (right) as observed in a 10 μm polyimide (PI) coated ITO cell (planar alignment) between crossed polarizers (arrows) on cooling at the indicated temperatures; the insets show the homeotropic samples at the same temperatures, as obtained between non-treated glass plates; for additional textures showing the SmA$^{(*)}$–SmA′$^{(*)}$–SmC$^{(*)}$ transitions, see Fig. S5 (ESI†).
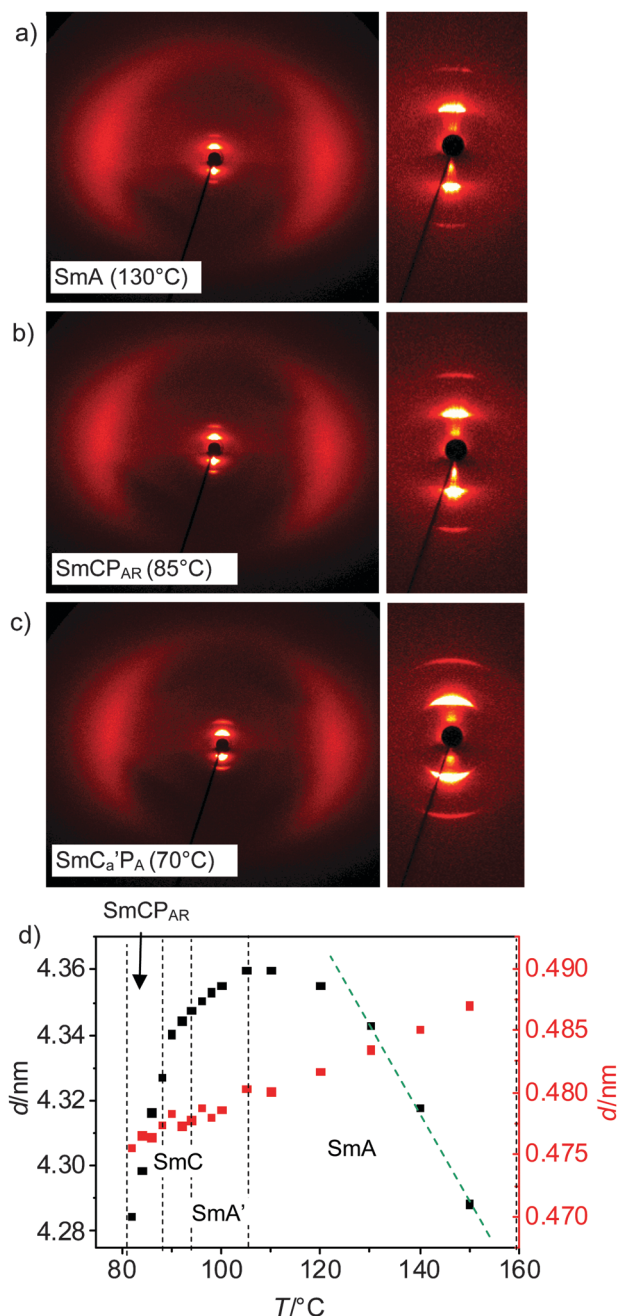
Fig. 5 (a–c) 2D-XRD patterns of an aligned sample of compound rac-2 in the distinct LC phases at the indicated temperatures; the left column shows the wide angle patterns, and the right column shows the patterns in the small angle region; (d) temperature dependence of the d-value of the small angle reflection (black) and the maxima of the diffuse wide angle scattering (red) in different mesophases (here crystallization takes place at 80 °C).

There is no change in the small- and wide-angle scattering until the phase transitions at $T = 81$ °C, where the layer reflection adopts a crescent-like shape (Fig. 5b and c). This would be in line with a small tilt of about 7°, though from the 2D-XRD patterns the presence of a tilt cannot be proven unambiguously. However, electro-optical investigations of planar samples (see Section 2.3.1) indicate a randomized or uniformly tilted organization in all LC phases below $T = 105$ °C.

The plot of the d-values of the small angle reflection depending on temperature indicates an increase of the layer spacing in the SmA range between $T = 157$ and 105 °C, in line with a growing packing density, leading to alkyl chain stretching. An increase of the packing density with decreasing T is supported by the observed increase of the birefringence of the planar fan texture, indicating a growing orientational order (Fig. 4a–c), and by the plot of the maximum of the wide angle scattering against temperature (see Fig. 5d, red dots), showing an almost linear reduction of the lateral intermolecular distances. In the SmA range between 179 and 130 °C the increase of the d-value of the layer reflection (black dots) is nearly linear and the slope starts decreasing at about 130 °C, the layer spacing reaches a maximum at $T = \sim105$ °C and then decreases. The decrease of the layer spacing could be caused by different reasons, among them an increase of the molecular bend[38] and a developing uniform or random tilt of the molecules with respect to the layer normal. There is a continuous and nearly linear decrease of d between 105 and 87 °C across the SmA–SmC transition temperature at $T = 93$ °C. This could mean that already in the SmA phase a random tilt of the molecules develops and therefore the phase range below $T \sim 105$ °C, designated as SmA′, can be considered as a de Vries type SmC phase[52] composed of small SmC domains which have a randomized tilt direction and grow in size with decreasing temperature. The tilt correlation remains short range until the continuous transition at $T = 93$ °C, where the tilt domains reach a critical coherence length, giving rise to phase biaxiality in the SmC phase. The de Vries character of the SmA′ phase range is further supported by the absence of a clear reduction of birefringence in the planar texture across the SmA′–SmC transition (see Fig. S5b and c, ESI†), confirming that the tilt should already be present in the SmA′ phase range, and by the observation of a field induced tilt in the SmA′(*) range (see Section 2.3.2).

2.2.2 LC phases of (S)-2. LC phase transition temperatures of enantiomer (S)-2 correspond to those of rac-2. Similar to rac-2 the fan texture of the SmA phase (Fig. 4d) breaks at $T = 93$ °C (Fig. 4e) and another significant change occurs at $T = 81$ °C (Fig. 4f). A major difference is between (S)-2 and rac-2 is observed at the phase transition at $T = 93$ °C where only for (S)-2 additional stripes develop perpendicular to the fans, being a sign of the development of a helical superstructure with a helical axis parallel to the layer normal (see Fig. 4e and Fig. S5f, ESI†).[53,54] In homeotropic samples birefringence appears at the SmA′*–SmC* transition at $T = 93$ °C (Fig. 4e). However, at some places pseudo-isotropic areas are retained in the SmC* phase or emerge in the SmCs′PF* range, due to the development of a helix structure, having a pitch close to the wavelength of light, but being still small enough to not reflect visible light (see the inset in Fig. 4f). These indications of a helical superstructure are not strictly associated with the phase transitions and are not uniform in the whole sample, indicating that the driving force for helix formation is obviously weak and strongly affected by competing surface effects.

2.3 Field-induced structures and electro-optical investigations

2.3.1 Electric field induced switching of the racemate rac-2. Under an applied triangular-wave field *rac*-**2** shows no current peak in the SmA, SmA′ and SmC phase ranges (up to 32 V$_{pp}$ μm^{-1}, see Fig. 6a), though optically a response on the field can be observed below T = 105 °C in the SmA′ range and in the SmC phase (Fig. 7a–c). The emergence of two broad polarization peaks in each period of the applied triangular wave voltage at T = 87 °C indicates the transition to the SmCP$_{AR}$ phase (Fig. 6b). With decreasing temperature the broad and widely separated peaks grow, continuously become sharper and move closer together on approaching the next phase transition at T = 81 °C (Fig. 6c and d).

This kind of broad double peak was previously observed for SmAP$_{AR}$[55] and SmCP$_{AR}$ phases.[36,37,56] Based on previous investigations of these kinds of SmCP$_{AR}$ phases there are small polar SmC$_s$P$_F$ domains having a preferred antipolar correlation.[37,57] Switching in this phase is assumed to be based on a Langevin process, where the small polar domains grow against thermal agitation under the applied field to form a polar SmC$_s$P$_F$ state, which relaxes back to the macroscopically antipolar polydomain ground state at E = 0 (Fig. 7j–l).[58] With lowering of the temperature the size of the polar domains grows and a lower threshold field is required for achieving a uniformly polar field-induced state, thus leading to the continuous merging of the two peaks (Fig. 6b–d). The polarization values continuously grow in the
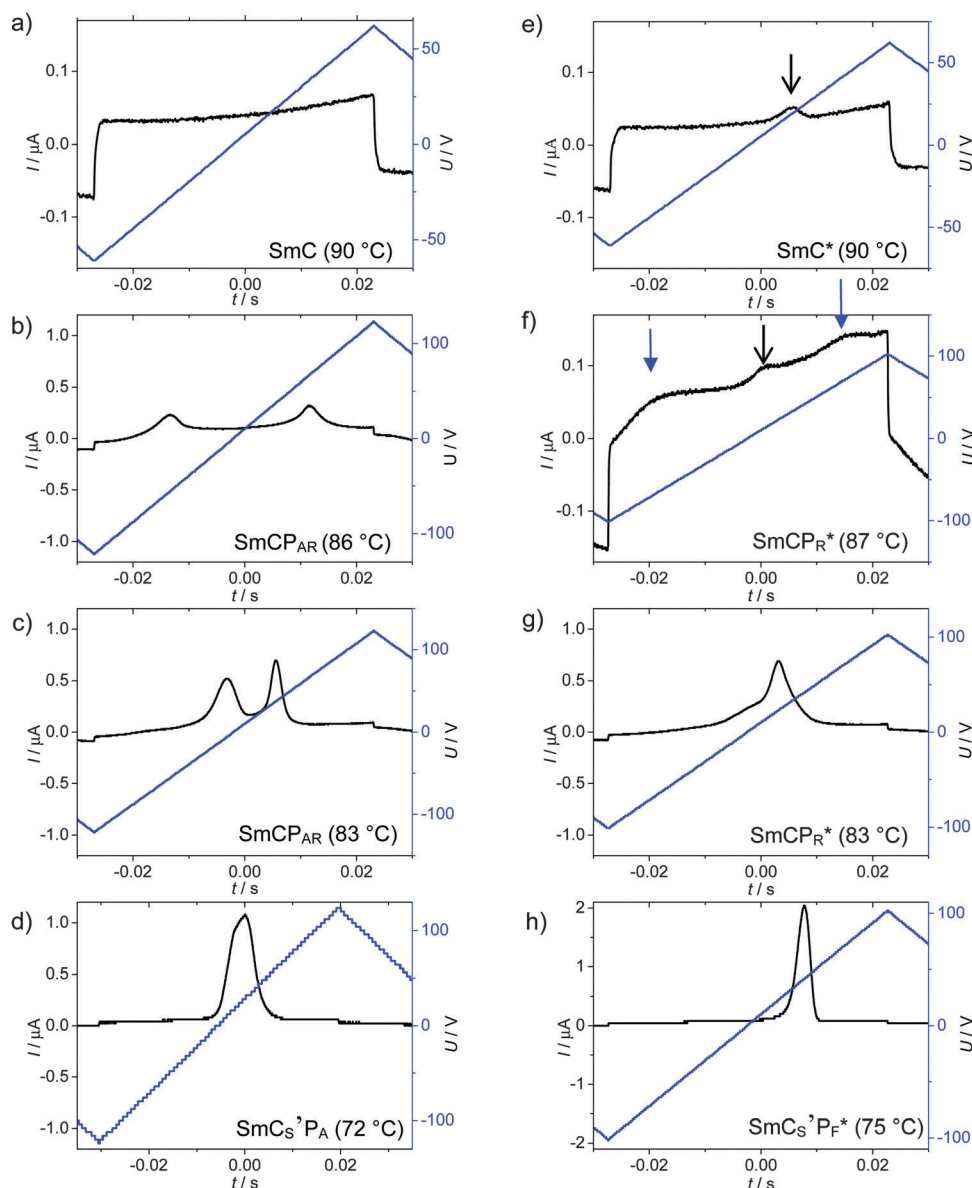

Fig. 6 Switching current responses obtained for (a–d) *rac*-**2** and (e–h) (*S*)-**2** under a triangular wave field (10 Hz, 5 kΩ) in a 6 μm ITO cell in the distinct phases at the indicated temperatures; please consider that different scales were used for the *P*-axis; additional switching curves are collated in Fig. S6 (ESI†) (*rac*-**2**, burst and field dependence in SmC$_s$′P$_A$), and Fig. S7–S9 (ESI†) ((*S*)-**2**, transition SmC*–SmCP$_R$* and burst in SmC$_s$′P$_F$*) and Fig. S10 (ESI†) ((*S*)-**2** and *rac*-**2** in SmC$_a$′P$_A$*) phases.
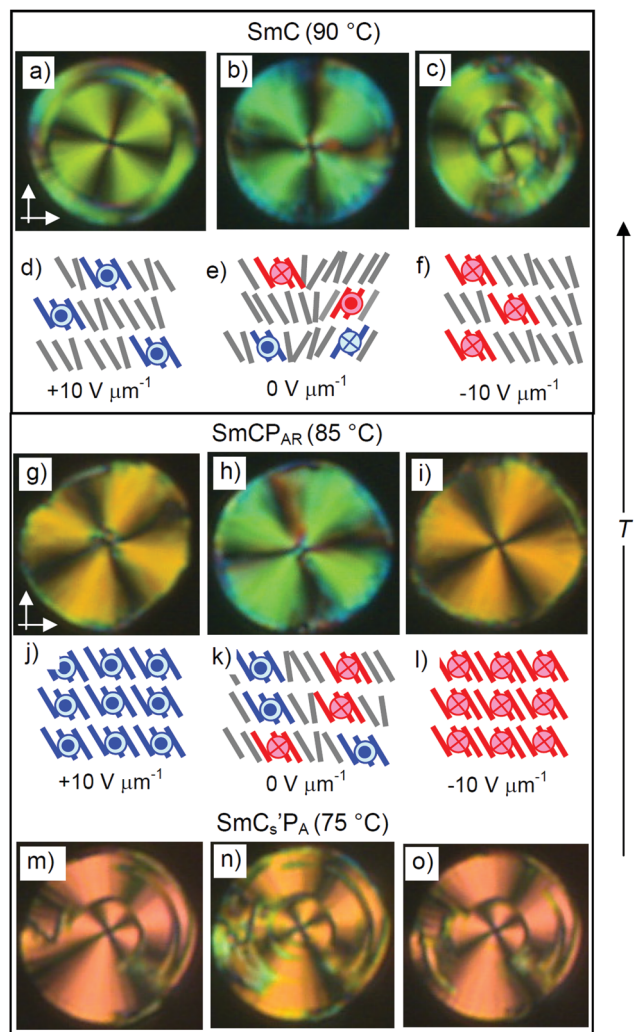
Fig. 7 Electro-optical investigation of compound *rac*-**2**. Textures of circular domains (a–c) in the SmC phase, (g–i) and in the SmCP$_{AR}$ phase and (m–o) in the SmC$_s$'P$_A$ phase as observed in a planar 6 μm ITO cell at the given temperatures and electric field strengths and models of the reorganization of the molecules under an *E*-field (d–f) in the SmC phase and (j–l) in the SmCP$_{AR}$, and SmC$_s$'P$_A$ phases, only the tilt domains at *E* = 0 would be much larger in the SmC$_s$'P$_A$ phase.
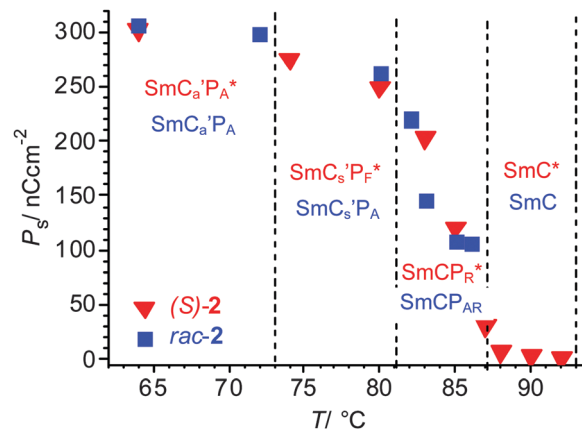

Fig. 8 Development of the spontaneous polarization in the smectic phases of *rac*-**2** and (*S*)-**2** depending on the temperature, for numerical data, see Table S1 (ESI†).

one half of the typical values observed for B$_2$-like SmCP$_A$ phases composed of polar layers ($\sim$600–800 nC cm^{-2}).[61] This suggests that none of the SmC phases of *rac*-**2** are formed by uniformly polar layers as known for the B$_2$ phases of the strongly bent type of bent-core mesogens, thus supporting a polar domain structure of these LC phases. For this residual domain structure a prime is added in the phase designation (SmC$_s$'P$_A$).

Optical investigations in planar cells (Fig. 7) provide information about the alignment and field-induced reorganization of the molecules in the smectic phases. In the SmCP$_{AR}$ and SmC$_s$'P$_A$ phases the direction of the dark extinctions is inclined with respect to the polarizer direction under an applied *E*-field and this orientation is retained after removing the applied field (Fig. 7g–i and m–o), indicating that a structure with a long range synclinic tilted organization is present under the electric field and that it is retained even after removal of the *E*-field. That the position of the extinctions does not change after field reversal means that the reorganization of the molecules takes place by inversion of only the polar direction, *i.e.* with inversion of the chirality of the field induced SmC$_s$P$_F$ states.

Though the field direction does not change the tilt direction, there is a significant effect of the electric field on the tilt angle in the SmA′, SmC and SmCP$_{AR}$ phases. The strongest effect is found in the SmC phase. Despite the phase biaxiality (Fig. 9), the extinctions in planar samples of the SmC phase are parallel to the polarizers in the absence of an applied field (Fig. 9e), which is attributed to the presence of anticlinic packing of the SmC domains. Inclination of the extinction crosses is induced under an applied *E*-field, rising with growing field strength until a saturation angle of $\sim$23° is reached (Fig. 9a and e–g), indicating a field induced tilt alignment. We attribute the steep increase of β at low *E*-field to the removal of any anticlinic packing and the further growth is attributed to the synclinic alignment of the tilt director of the SmC$_s$P$_F$ domains in the SmC$_s$P$_F$ state developing under the *E*-field, due to the inherent coupling between the polarization direction and the tilt direction (Fig. 9a). The coexistence of areas with extinction crosses of the opposite direction (Fig. 7 and 9g) indicates that a macroscopic
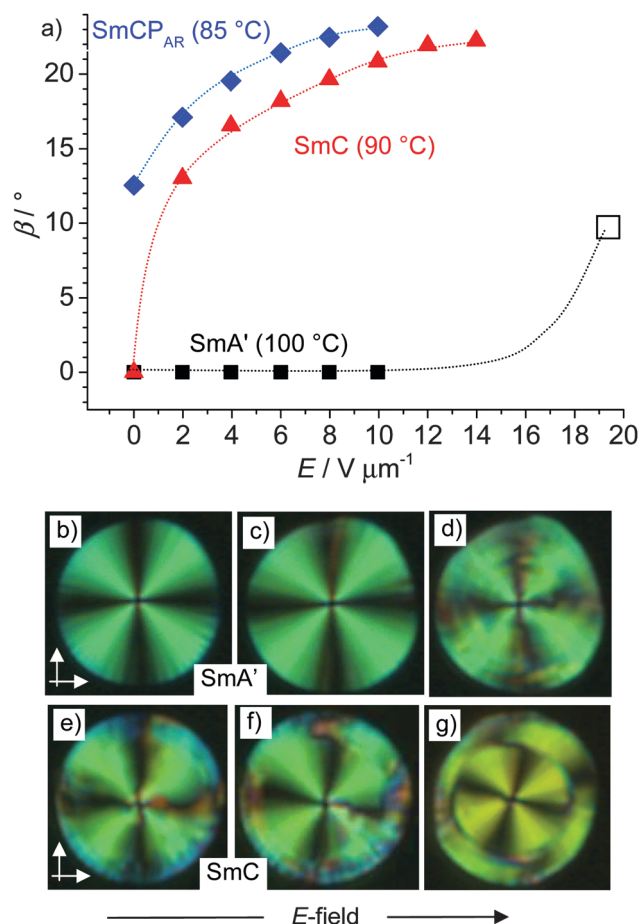
SmCP$_{AR}$ range and reach 200–220 nC cm^{-2} at the next phase transition to the SmC$_s$'P$_A$ phase at *T* = 81 °C (Fig. 8).

At this discontinuous phase transition a relatively broad and non-symmetric "single" peak is formed (Fig. 6d) which is positioned close to zero voltage crossing and splits into two if a modified triangular wave voltage with an additional relaxation time at 0 V is applied (Fig. S6b, ESI†).[59] Therefore, the single peak does not indicate ferroelectric switching. The switching appears to represent a kind of superparaelectric switching[60] where relatively large SmC$_s$P$_F$ domains merge by formation of a field-induced macroscopic polar SmC$_s$P$_F$ structure and relax back to an apolar polydomain structure around *E* = 0 (similar to Fig. 7j–l). The polarization reaches a value of *P*$_s$ = 270 nC cm^{-2} in the SmC$_s$'P$_F$* range and 300 nC cm^{-2} in the SmC$_a$'P$_A$* phase before crystallization (Fig. 8), which is only about one third to

Fig. 9 (a) Field strength dependence of the optical tilt angle β of *rac*-**2** in the distinct smectic phases; $\square$ indicates the roughly estimated value from (d); in the SmC$_s$'P$_A$ phase the tilt is field-independent and amounts to $\sim$30° (see Fig. 7m–o); the accuracy of the tilt angle measurements is in the range of $\pm$2°; (b–d) circular domains in the SmA' phase at (b) $E = 0$, (c) $E = 12$ V μm^{-1} and (d) $E = 20$ V μm^{-1} and (e–g) in the SmC phase at (e) $E = 0$, (f) $E = 2$ V μm^{-1} and (g) $E = 12$ V μm^{-1}; white arrows show the orientation of the polarizers.

mixture of oppositely tilted, and hence oppositely chiral, SmC$_s$P$_F$ areas is formed under the applied field.

In the SmCP$_{AR}$ phase a synclinic tilt of 12–13° is found already at $E = 0$ (Fig. 7h), indicating a preference for synclinic SmC$_s$P$_F$ domain correlation even in the absence of an E-field and the tilt increases with growing field strength to about 22°, which is approximately the same value as that found in the SmC phase (Fig. 9a). In the SmC$_s$'P$_A$ phase the tilt is significantly larger ($\sim$30°) and no field dependence is observed (Fig. 7m–o). No tilt is found in the SmA phase at the highest temperature, though below $T = 105$ °C in the SmA' range a tilt of $\sim$10° is induced at a relatively high field strength of ≥ 20 V μm^{-1} (Fig. 9a and d).[62] This supports the proposed de Vries like SmC (and field induced SmC$_s$P$_F$) domain structure of the uniaxial smectic phase in the SmA' range.

2.3.2 Electro-optical investigation of the enantiomer (*S*)-2

SmA' * phase.* For enantiomer (*S*)-**2** an E-field induced change in the position of the extinction crosses is found in circular

domains in the SmA'* range below $T = 105$ °C. Even under weak E-fields the extinction crosses rotate from being aligned parallel to inclined with respect to the polarizer direction, indicating the induction of a synclinic tilted organization of the molecules which is inverted by field reversal (Fig. 10a–c). The tilt angle increases almost linearly with field strength (Fig. 11) and also increases with decreasing temperature. Because no tilt is observed under the same conditions ($E < 15$ V μm^{-1}) in the SmA' phase region of racemate *rac*-**2** (see Fig. 9a–c) the effect is assigned to an electroclinic effect due to the coupling of molecular chirality with tilt. However, such a strong electroclinic effect is unexpected for a compound having "weakly chiral"
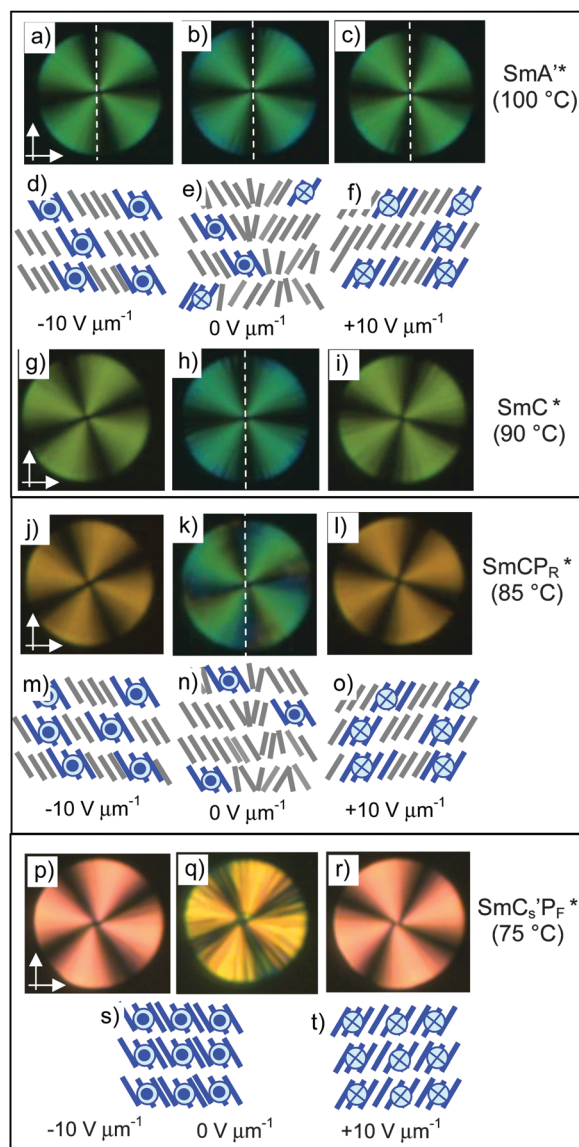

Fig. 10 Electro-optical investigation of the enantiomer (*S*)-**2**. Circular domain as observed between crossed polarizers (white arrows), (a–c) in the SmA'* phase, (g–i) in the SmC* phase, (j–l) in the SmCP$_R$* phase and (p–r) in the SmC$_s$'P$_F$* phase as observed in a planar 6 μm ITO cell under the indicated E-fields and models showing the field induced reorganization of the molecules (d–f) in the SmA'* and SmC* phases, (m–o) in the SmCP$_R$* phase and (s and t) in the SmC$_s$'P$_F$* phase.

stereogenic centers in the branched alkyl chains. This suggests that the de Vries-like local $SmC^{(*)}$ domain structure contributes to the observed effect. A sufficiently large dipole moment, being addressable by the E-field should result from the sterically induced polar order arising from the restriction of molecular rotation around the long axis (evolving P_b) under the E-field, thus leading to a polarization of the $SmC^{(*)}$ domains with transformation to polar $SmC_SP_F^{(*)}$ domains. Only at high E-field (20 V μm^{-1}) a sufficiently large polarization is achieved without the support of molecular chirality in the SmA$'$ phase of rac-**2**, leading to a tilt comparable with that in the chiral SmA$'*$ phase of (S)-**2**. In contrast to rac-**2**, where areas with opposite tilt directions occur simultaneously, for the enantiomer (S)-**2** the chirality–tilt-coupling leads to a uniform tilt in the whole sample, i.e. all extinction crosses have the same direction. The coupling of the tilt with the polar direction leads to a preferred synpolar coupling between the $SmC_SP_F^*$ domains which provides cooperativity and allows a response to much weaker E-fields. So the electroclinic effect in the SmA$'*$ phase of (S)-**2** is essentially chirality based, but nevertheless, it is supported by the developing P_b. The SmA$'$ phase of rac-**2**, lacking the chirality coupling, requires much higher field strength for tilt alignment. Both cases do not represent classical electroclinic effects[4] where orthogonally organized molecules tilt under the applied field, instead it is considered as a field induced alignment of an already existing, but randomized tilt.[62,63] There is no visible polarization current peak, indicating a dielectric response in the SmA$'$ and SmA$'*$ phase ranges.

SmC* phase. A single current peak with a small polarization value (P_s = 1–7 nC cm^{-2}), being positioned significantly after 0 V crossing (no splitting is observed under a modified triangular wave field with waiting time at 0 V),[64] develops at T = 93 °C indicating a ferroelectric switching of the SmC* phase (see the black arrow in Fig. 6e). The small polarization value corresponds to those expected for SmC* phases of rod-like molecules with the same kind of chiral alkyl chain.[46] Moreover, there is no field strength dependence of the polarization, indicating independence from the $SmC_SP_F^*$ domain size and therefore it could be attributed to a chirality induced ferroelectric switching based on P_c. Optical investigations under a DC field indicate a relaxation to a ground state with the extinctions being parallel to the polarizers (Fig. 10h). This is attributed to tilt randomization with some preference for anticlinic packing of the $SmC_SP_F^*$ domains at E = 0, as also found for the SmC phase of rac-**2**. A synclinic alignment of the $SmC_SP_F^*$ domains is achieved under an applied E-field; with growing field strength the order parameter, and hence the average tilt angle is increased until a saturation value is reached at $\beta \sim 22°$ (see Fig. 11).[65] Though there is a uniform tilt, the polar coherence length in the SmC* phase is obviously still not large enough that P_b can be directly addressed by the applied electric field and only switching of P_c is observed. Nevertheless, the significant increase of P_s from 1 to 7 nC cm^{-2} in a small temperature range might indicate an emerging coupling between P_c and P_b with decreasing temperature.
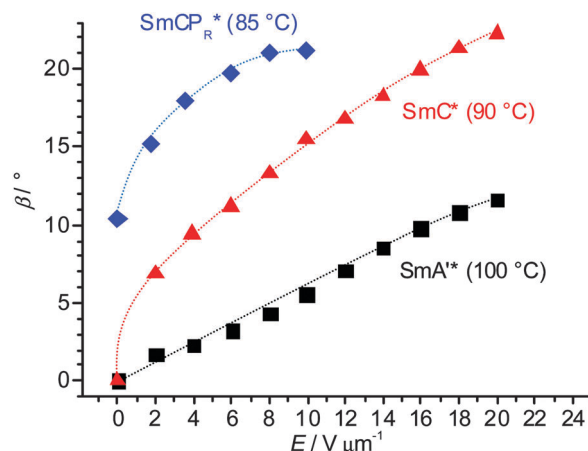

Fig. 11 Field strength dependence of the optical tilt of (S)-**2** in the distinct smectic phases (average of the amounts of right and left tilt of two measurements); in the $SmC_S'P_F$ phase the tilt is field-independent and amounts to ∼30° (see Fig. 10p–r); the accuracy of the tilt angle measurements is in the range of ±2°.

SmCP$_R$* phase. Two broad peaks start developing at T = 87 °C at the transition to the next phase, designated as SmCP$_R$* (blue arrows in Fig. 6f), indicating that at this temperature the $SmC_SP_F^*$ domains have reached a critical size allowing the formation of sterically induced polar order (P_b) under a reasonable threshold field. However, the growing polar domain size and polarization also favor the antipolar coupling between the $SmC_SP_F^*$ domains, thus leading to antiferroelectric-like switching, as observed for the $SmCP_{AR}$ phase of racemate rac-**2** (see previous section). Formation of the broad double peak is only temporary and on further cooling a single peak rapidly grows at the expense of the double peak (black arrow in Fig. 6f, see also Fig. 6g and Fig. S8, ESI†), thus changing the switching from antiferroelectric-like (SmCP$_{AR}$*) to ferroelectric-like (SmCP$_R$*). It is proposed that the increasing strength of coupling between molecular chirality and SmC_SP_F layer chirality at lower temperature stabilizes the synpolar order and removes antipolar packing. Thus, the $SmCP_{AR}$ phase of the racemate is replaced by a SmCP$_R$* phase for the enantiomer (S)-**2** (Fig. 10j–o).[57] Also in the SmCP$_R$* phase there is a field induced increase of tilt approaching a plateau at ∼22° tilt (Fig. 11), just like in the $SmCP_{AR}$ phase of the racemate (Fig. 9a), being in line with the proposed Langevin-type switching.

SmC$_S$$'P_F$* phase. A sharp single switching peak per half period of the triangular wave voltage is observed below T = 81 °C. In contrast to the broad "single peak" in the $SmC_S'P_A$ phase of rac-**2**, the peak is sharper and appears significantly after 0 V crossing (Fig. 6h). The polarization peak is symmetric in the whole temperature range and does not split under a modified triangular wave voltage (see Fig. S9, ESI†), excluding superparaelectric switching[60] or a field induced helix deformation,[45,66] thus being an indication of ferroelectric switching.[67] Optical investigations in the temperature range of the $SmC_S'P_F^*$ phase confirm bistable switching between two polar states (Fig. 10p–t).

Because diasteromeric relationships of the SmC_SP_F domains with fixed molecular chirality lead to a reduced energy of the preferred $SmC_SP_F^*$ state (matched case), it is stabilized and can be retained even at 0 V, and this leads to ferroelectric switching. The position of the extinctions is opposite in the two switched states (see Fig. 10p and r and 12e and h), confirming a switching by rotation on the tilt cone for (S)-2. The spontaneous polarization and the dependence of P_s on temperature are nearly identical for rac-2 and (S)-2, both reaching $P_s = 250–270$ nC cm^{-2}, thus indicating that there is no visible contribution of P_c to the total polarization (see Fig. 8).[68] These polarization values are comparatively small for a bent-core molecule, confirming that the residual polar domain character is also retained for the homogeneously chiral compound and that there is no significant effect of chirality on the domain size and polarization itself. The main effects of molecular chirality are the induction of ferroelectric switching in the SmC* phase due to coupling between molecular chirality, tilt and polarization, and the change in the switching from tristable modes of Langevin-like ($SmCP_{AR}$) and superparaelectric switching ($SmC_s'P_A$) to bistable (ferroelectric) modes in the corresponding $SmCP_R^*$ and $SmC_s'P_F^*$ phases.
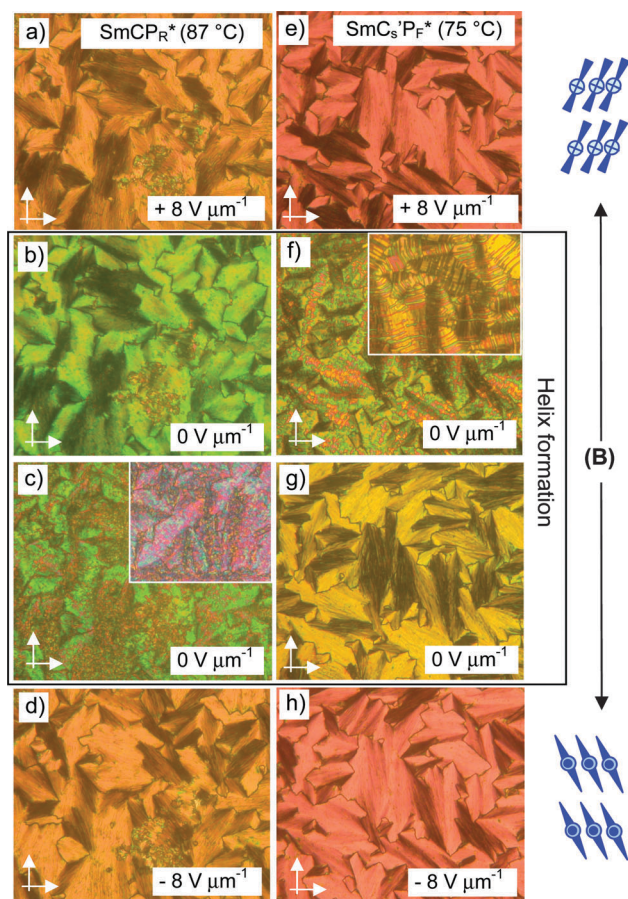

Fig. 12 Texture of the LC phases of compound (S)-2 in a 10 μm PI-coated ITO cell at the given temperatures and electric field strengths (a–d) in the $SmCP_R^*$ phase and (e–h) in the $SmC_s'P_F^*$ phase; (b) and (f) were observed immediately after switching off the applied field (ca. 1 s) and those in (c and g) after ca. 5 s; the inset in (c) shows the texture after ca. 20 s and the inset in (f) shows the texture after 5 s at +0.8 V μm^{-1}.

2.3.3 Helical superstructures in the LC phases of the enantiomer (S)-2.

It is known that homogeneously chiral stereogenic centers in the molecules provide some bias to the transiential helical molecular conformations.[69] Because in soft matter systems helical molecules cannot align strictly parallel to each other, but only with a small twist between adjacent molecules, chirality is inevitably associated with a helical twist. For compound (S)-2 a helical twist with the helical axis parallel to the layer normal occurs at the transition from the SmA'* to the SmC* phase, as indicated by the stripe pattern occurring perpendicular to the fans in the planar textures (Fig. S5f, ESI†),[53] and by the often-observed optical uniaxiality of the homeotropic samples. Helical organization is also found in the pristine ground states of the $SmCP_R^*$ and $SmC_s'P_F^*$ phases (Fig. 4e and f) and it is removed under the applied electric field.

A large difference in birefringence between the field-on and field-off states in the $SmCP_R^*$ and $SmC_s'P_F^*$ phases of (S)-2 (see Fig. 12) is observed in 10 μm PI-coated ITO cells. This is not found in 6 μm cells (Fig. 10) and also not for the $SmCP_{AR}$ and $SmC_s'P_A$ phases of the achiral racemate rac-2 (see Fig. 7). Therefore, it is assigned to the development of a chirality induced helical modulation of the tilt direction after removal of the alignment field. In the $SmCP_R^*$ phase of (S)-2 the position of the extinctions is inclined with respect to the direction of the polarizers in the field induced $SmC_SP_F^*$ state and this is retained at 0 V, though a significant decrease of birefringence is observed (color change from orange to green, see Fig. 12a and b). The birefringence slowly decreases further (pink/blue), and the extinctions become aligned parallel to the polarizers after a few (~10–20) seconds (see Fig. 12c inset). It appears that immediately after switching off the applied field only a local modulation of the tilt direction takes place, meaning that helix formation in the $SmCP_R^*$ phase is obviously a slow process. In the $SmC_s'P_F^*$ phase at lower temperature relaxation almost immediately leads to a flipping of the extinctions to positions parallel to the direction of the polarizers (Fig. 12f) and a smooth texture with reduced birefringence (yellow) is formed quickly (Fig. 12g),[70] indicating that the driving force for helix formation is stronger.

2.3.4 Anticlinic low temperature phase of rac-2 and (S)-2.

Finally we would like to briefly discuss the low temperature phases occurring below $T = 73$ °C for the racemate as well as for the enantiomer of compound 2 (Fig. 13). There are textural changes at this temperature, which are most clearly observable in 6 μm cells, known to suppress helix formation (see above). For (S)-2 a slow relaxation of the field induced SmC_SP_F state to a low birefringent texture with the extinction crosses parallel to the polarizers is observed after switching off the applied field (Fig. 13b and c).

For the racemate the same transition is found, but in this case it takes place immediately after switching off the field without any delay (Fig. 13f and g). As the same textural changes were found for the enantiomer as well as for the racemate, it is unlikely that helix formation could be mainly responsible. A transition from a synclinic to an anticlinic phase structure is the likely reason for this textural change.[71] Accordingly, a
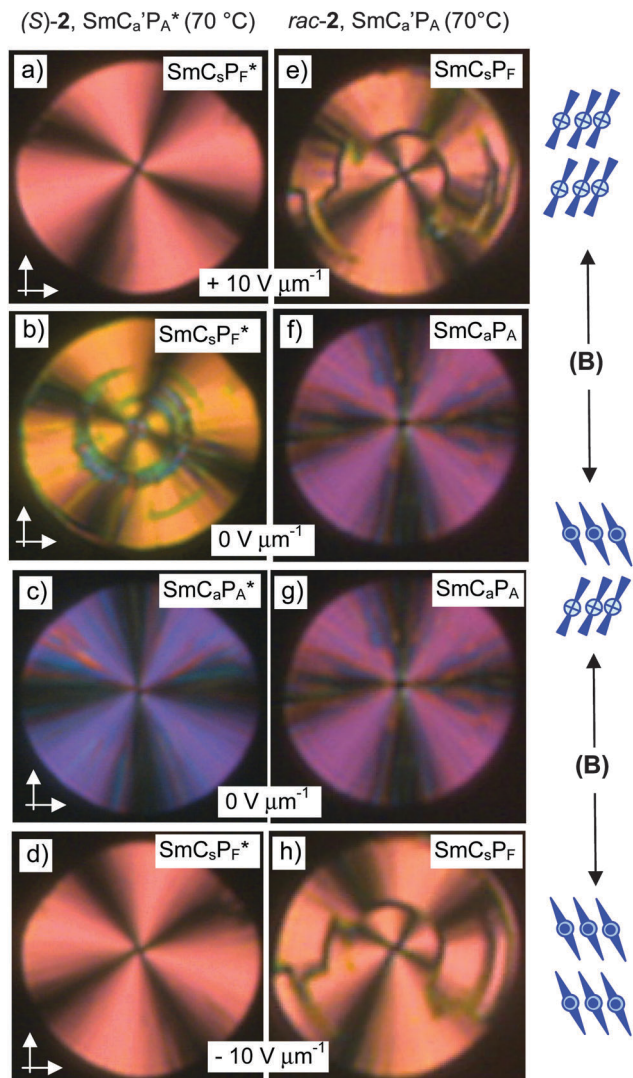
(S)-**2**, SmC$_a$'P$_A$* (70 °C)   rac-**2**, SmC$_a$'P$_A$ (70°C)

Fig. 13 Textures of the low temperature SmC$_a$'P$_A^{(*)}$ phases (a–d) of (S)-**2** and (e–h) of rac-**2** in a 6 μm ITO cell at the given temperatures and electric field strengths (b) and (f) were observed immediately after switching off the applied field and those in (c and g) after ca. 10 s.

relaxation to a non-polar SmC$_a$P$_A^{(*)}$ state takes place by rotation on the tilt cone for the racemate as well as for the enantiomer (see Fig. 14d and h), thus retaining a homogeneous layer chirality. Though the tilt correlation in the ground state changes at $T = 73$ °C, there is no change in the number and shape of the current peaks (Fig. S10, ESI†) and no jump in the P_s values (see Fig. 8), i.e. there is obviously no effect of the changing tilt correlation on the type of switching, being superparaelectric for rac-**2** and ferroelectric for (S)-**2**. Therefore we conclude that this low temperature SmC phase still retains some residual domain character (indicated by the prime in the phase designation), but the polar domains have exceeded a critical size at which the emerging antipolar interlayer interfaces become dominating for the optical properties (see discussion in the Summary and conclusions section). Whereas the transition from the field induced SmC$_s$P$_F^{(*)}$ state to the non-polar SmC$_a$P$_A^{(*)}$ structure is fast for the racemate, it is slow
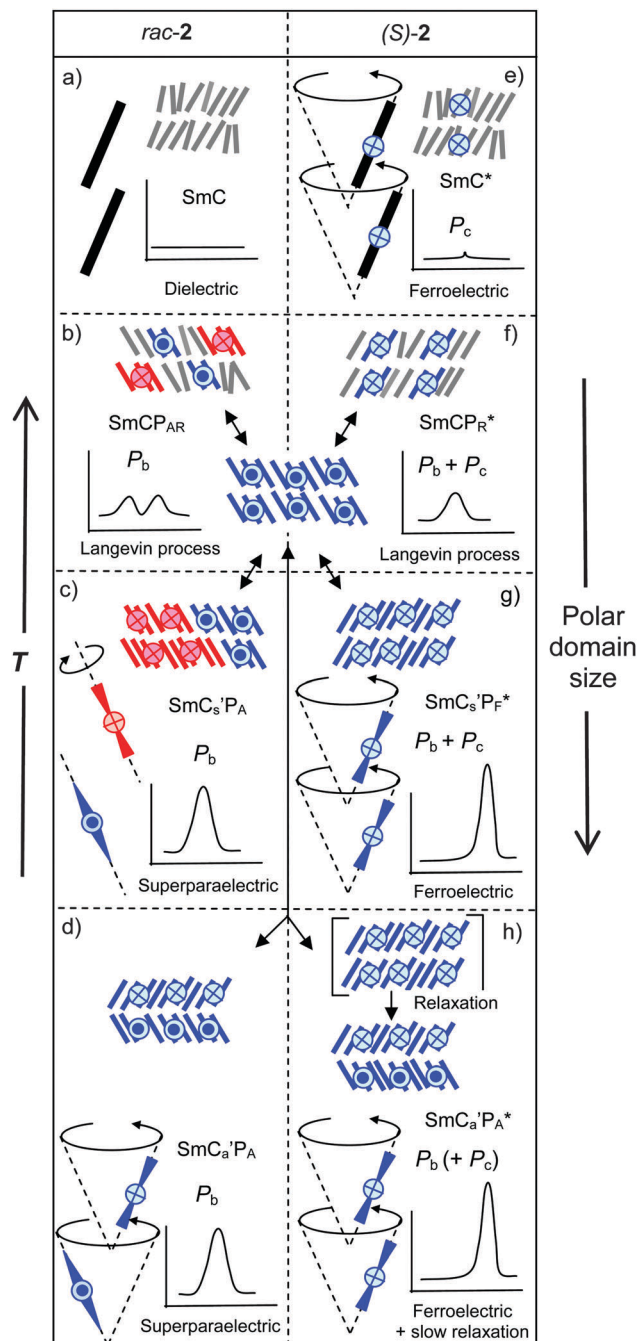

Fig. 14 Summary of phase structures, shapes of polarization curves and modes of E-field induced switching in the distinct SmC phases of compound **2**; color distinguishes the sense of the superstructural layer chirality.

for (S)-**2**. Thus it appears that in the case of (S)-**2** the polar SmC$_s$P$_F$* state is still stabilized by the chirality–tilt-coupling, supporting synpolar correlation of SmC$_s$P$_F$* domains and making this relaxation slow. On the other hand, in anticlinic phases the chirality–tilt-coupling stabilizes the antipolar order as known for the SmC$_A$* phases of chiral rod-like LCs.[4] The SmC$_a$'P$_A$* phase of (S)-**2** appears to be just at the cross-over from synpolar to antipolar organization. Chirality–tilt-coupling is still stabilizing the field induced SmC$_s$P$_F$* state, thus retaining ferroelectric

switching and delaying the relaxation process, whereas at $E = 0$ the SmC$_a$P$_A$* structure, governed by the emerging anticlinic interlayer interfaces, becomes dominating. Despite the ferroelectric switching of the field-induced SmC$_s$P$_F$* states we choose the phase designation SmC$_a$'P$_A$*, describing the most stable ground state structure.

2.4 Discussion of relationships between the molecular structure, polar order, chirality and mode of switching

A summary and comparison of the proposed phase structures and switching behavior of compound **2** depending on the chirality and temperature is shown in Fig. 14. In order to generalize the effects of chirality on the self-assembly of bent-core mesogens we consider here the previously reported case of compound **1** (see Fig. 2), having two biphenyl wings replacing the terephthalate units in compound **2**.[29] Both compounds **1** and **2** show a high temperature SmA phase followed by different SmC$^{(*)}$ phases (Fig. 2 and Table 1). In both cases the high temperature SmC phase is non-polar whereas the enantiomers have ferroelectric SmC* phases with bistable switching by rotation on a cone (Fig. 14e and 15c). The SmC* phase of (S)-**1** does not show any visible polarization peak, confirming the absence of P_b, whereas the small polarization peak in the SmC* phase and the electroclinic effect in the SmA'* phase of (S)-**2** indicate an emerging contribution of P_b.

There are significant differences for the polar low temperature SmC$^{(*)}$ phases following the SmC$^{(*)}$ phase. The low temperature phases of rac-**1** and (S)-**1** both show antiferroelectric switching indicated by two sharp and well-separated polarization current peaks per half period of the applied triangular voltage and having a high P_s value ($P_s = 700–800$ nC cm^{-2}) as typically observed for bent-core mesogens and there is no effect of molecular chirality on the switching mechanism (Fig. 15b and d). Optical investigations indicated that the field induced polar SmC$_s$P$_F$$^{(*)}$ states relax to a racemic apolar SmC$_s$P$_A$$^{(*)}$ structure by rotation around the long axis (**A**), which reverses the superstructural chirality (Fig. 15b and d). This means that the low temperature smectic phase behaves like a typical B$_2$ phase of a bent-core mesogen. For (S)-**1** where the molecular chirality is uniform, this switching leads to two energetically different diastereomeric field-induced SmC$_s$P$_F$* states, depending on the direction of the applied electric field. The less stable SmC$_s$P$_F$* state (mismatched case) slowly relaxes under the applied field, where tilt flipping with constant polar direction (process (**C**) in Fig. 1b) leads to the formation of the more stable diastereomeric state (matched case, see Fig. 2b). This kind of slow reorganization process cannot be observed for (S)-**2**, because the switching takes place by rotation on a cone which retains the superstructural layer chirality once developed, and thus the field induced state always represents the energy minimum diastereomer. This indicates that compared to compound **2** the coupling between molecular and superstructural chirality is much weaker for compound **1** and thus in this case chirality can neither induce ferroelectric switching in the polar smectic phases nor it can change the mode of switching from a rotation around the long axis to the chirality retaining rotation on a tilt-cone. As another difference, there is an abrupt transition from the behavior as a typical rod-like molecule to typical bent-core behavior for compound **1** whereas for compound **2** this transition is smooth and a true B$_2$-like phase is never achieved. The very distinct behavior of compounds **1** and **2** must be due to the change in the structure and the length of the rod-like wings by introduction of the COO linking unit. The rigid biphenyl wings in compound **1** obviously lead to a pronounced bent molecular shape at reduced temperatures, being responsible for polar packing, hence, in this case polar order is dominated by P_b. The terephthalate wings in compound **2**, being more flexible, provide improved attractive intermolecular interactions and, due to the increased molecular length, probably also an increased nematic order parameter, which do not lead to an abrupt change from non-polar to polar smectic phases. For this compound the balance between the molecular shape and the intermolecular interactions obviously contributes to a continuous development of polar order with decreasing temperature. In this case diastereomeric relationships have a significant impact on the polar packing of the bent cores, i.e. molecular chirality leads to ferroelectricity and rotation on a cone.

The bent-core compound **3**, reported by Sadashiva et al.,[28] behaves very similar to compound **1** (see Table 2). The high temperature smectic phases (SmC$_s$, SmC$_a$) of the racemate rac-**3** are non-polar and the enantiomer (S)-**3** shows chirality induced ferroelectric switching on a cone in the SmC$_\gamma$* and SmC* phases (see Fig. 15a and c). The low temperature phase has a racemic SmC$_s$P$_A$$^{(*)}$ structure, in this case with additional
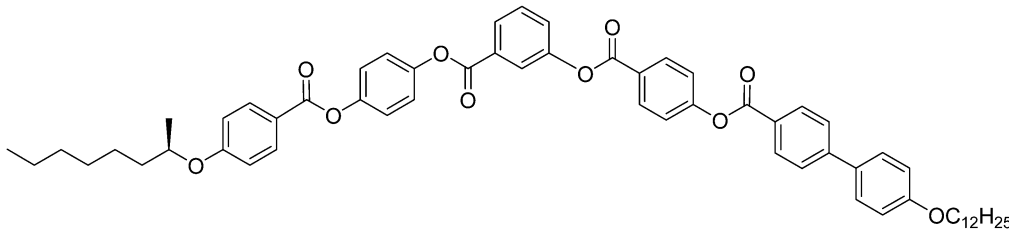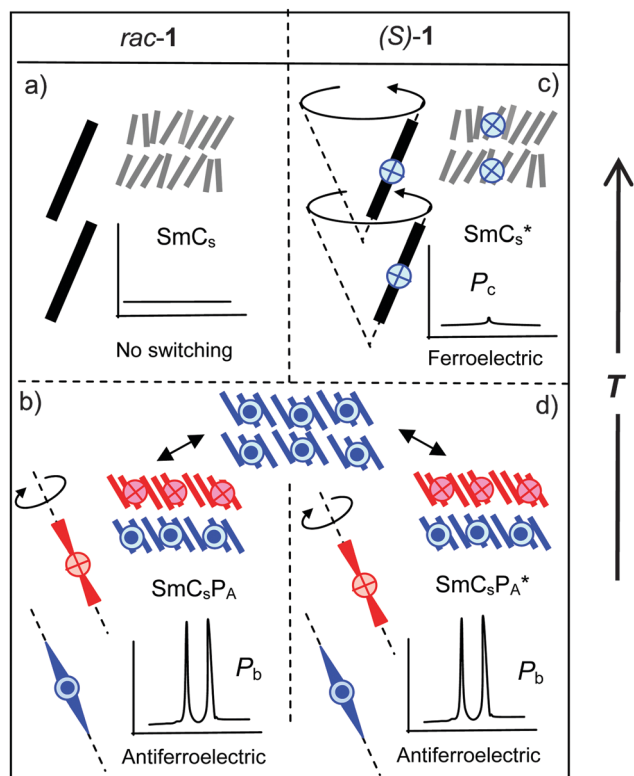

Fig. 15 Summary of phase structures, shapes of polarization curves and modes of electric field induced switching in the distinct SmC phases of compound **1**.[29] In principle, the same scheme can be applied for the SmC phases of compound **3**.[28]

Table 2 Comparison of mesophases and phase transition temperatures of the racemic compound *rac*-**3** and its (*R*)-enantiomer[28][a]

	$T/°C$ [ΔH kJ mol^{-1}]
rac-**3**	Cr 114 SmC̃$_s$P$_A$ 118 SmC$_s$ 142 SmC$_a$ 148 X 148.5 Iso
(*R*)-**3**	Cr 115 SmC̃$_s$P$_A$* 118 SmC$_\gamma$* 141 SmC* 147 X* 148 Iso

[a] SmC$_\gamma$* = ferrielectric switching tilted smectic phase; SmC̃$_s$P$_A$[(*)] = modulated synclinic tilted and antiferroelectric switching smectic phase (Col$_{ob}$P$_A$[(*)] phase); X[(*)] = non-specified biaxial smectic phase.

in-plane modulation (SmC̃$_s$P$_A$[(*)]). There is P_b-based antiferro-electric switching around the long axis with two well separated peaks and high polarization values (see Fig. 15b and d). Only the relaxation process by flipping of the layer chirality (process (**C**) in Fig. 1b, see also Fig. 2b), found for (*S*)-**1**, was not reported for (*S*)-**3**, probably it is inhibited by the layer modulations in this case.

Finally we would like to include the bent-core compound (*S*)-**4**,[16] with a strongly bent core involving Schiff base units, reported by Takezoe *et al.*, in the discussion. This compound and related compounds were only synthesized as uniformly chiral (*S,S*)-enantiomers and therefore no direct comparison with the racemate is possible in this case. For (*S*)-**4** different field-induced and ground state structures coexist and ferro-electric switching takes place by rotation on a cone with high polarization values. The racemic SmC$_a$P$_F$* state was identified as one of the stable ground state structures[18] and under an applied field SmC$_s$P$_F$* states with either handedness coexist with the racemic SmC$_a$P$_F$* state.[16] It appears that in this case there is no coupling between molecular chirality and layer chirality. If ferroelectric switching is induced by the molecular chirality or by the modification of the interlayer interfaces due to the presence of chain branching cannot be decided, as the behavior of the related racemate is unknown in this case.

tilt, a reduction of the importance of anticlinic tilt correlation and a change in the switching from rotation on a tilt cone to the rotation around the molecular long axis.[72]

3. Summary and conclusions

A 4-cyanoresorcinol based bent-core molecule with two tere-pthalate wings and two chiral 3,7-dimethyloctyloxy chains was synthesized as a pure (*S,S*)-enantiomer and as an optically inactive racemic mixture, and both were investigated with respect to the effects of chirality on LC phase formation and switching under an electric field.

Below 105 °C there is a tilt in all LC phases, only the coherence length of the tilt is different, being short range in the SmA$'$[(*)] phase and long range in the distinct SmC[(*)] phases. At high temperature this compound behaves like a rod-like molecule with its properties dominated by the polarization induced by molecular chirality (P_c), leading to ferroelectric switching in the SmC* phase and a significant electroclinic effect in the SmA$'$* phase of enantiomer (*S*)-**2**. At lower tem-perature the rotation around the molecular long axis becomes restricted, giving rise to the simultaneous development of

(*S*)-**4**: Iso 167 SmC$_a$P$_F$* 146 SmY* 138 B3* ($T/°C$ on cooling)[16]
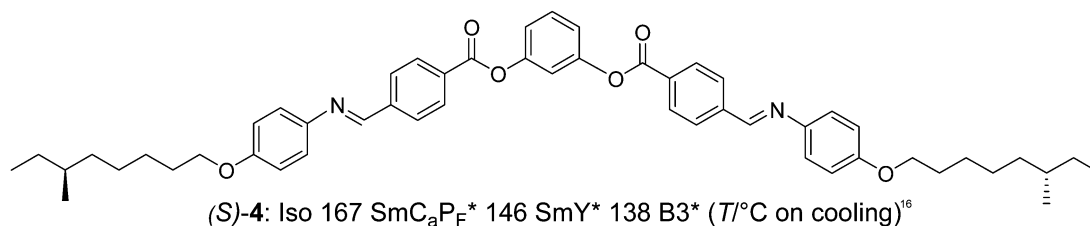
Overall it appears that the coupling between molecular chirality and supramolecular chirality in polar SmC[(*)] phases increases in the order **4** < **3** < **1** < **2**. In the same order the molecular shape changes from a typical bent-core mesogen (compound **4**) to a weakly bent molecule (compound **2**) and the contribution of P_b decreases. This molecular structural change is associated with a transition form long range polar order (polar layers) to local polar order in domains, a reduction of the

sterically induced polar order (P_b) and superstructural layer chirality. These smectic phases are considered as being composed of small SmC$_s$P$_F$ domains preferring an antipolar correlation which leads to the macroscopically polarization randomized SmCP$_{AR}$ and SmC$_s'$P$_A$ phases for *rac*-**2**.[57] The field induced alignment of these SmC$_s$P$_F$ domains leads to non-classical electroclinic effects in the SmA$'$, SmC[(*)] and SmCP$_{(A)R}$[(*)] phases of *rac*-**2** and (*S*)-**2**.[63] For *rac*-**2** the tilt direction is retained

by reversing the applied field which is attributed to surface alignment effects (SmC) and rotation around the long axis (SmC$_s$′P$_A$ and SmCP$_{AR}$).

In the LC phases of the uniformly chiral compound (*S*)-**2** additional diastereomeric relationships between the fixed molecular and the transiential superstructural chirality of the SmC$_s$P$_F$ domains lead to energetically different pairs with the more stable being preferred, thus fixing just one specific combination of the tilt direction and the polar direction. For this reason the tilt is uniform under an applied *E*-field and it is inverted by field reversal, thus retaining the once developed energetically favored diastereomeric pair by reorganization *via* rotation on the tilt cone. Because a uniform synclinic tilt is present, a uniform direction of polarization is inevitably stabilized due to the coupling of the tilt direction and the polar direction, thus leading to ferroelectric and ferroelectric-like switching in the SmC$_s$′P$_F$* and SmCP$_R$* phases of (*S*)-**2**, respectively. This coupling of P_b with molecular chirality provides new access to high polarization ferroelectric LC materials by utilizing molecules combining a weak molecular chirality with a weakly bent core structure. The polarization is almost the same in *rac*-**2** and (*S*)-**2** which shows that polarization is determined by P_b and means that the domain size and the magnitude of polarization are not affected by molecular chirality, it only removes the antipolar domain correlation. Investigation of the low temperature SmC$_a$′P$_A$* phase of compound **2** and a comparison of the phase sequence of this compound with related chiral bent-core molecules (compounds **1**, **3** and **4**) indicate that a further increase in the molecular bend and growing polar order (increasing contribution of P_b) obviously favour anticlinic and antipolar SmC phases and reduce the influence of molecular chirality. This means that only for weakly bent molecules can the molecular chirality support synpolar order. The reason might be that for rod-like or weakly bent molecules synclinic tilt is inherently preferred by interlayer fluctuations (providing an entropic gain). However, these fluctuations favor an antipolar packing of the molecules in adjacent layers if a molecular bend emerges and increases (Fig. 16).[71] For strongly bent molecules the effects of the competing interlayer interfaces become dominating, obviously overriding the effects of molecular chirality on tilt and polarization and thus leading to a preference for antiferroelectric phases, even for the enantiomers.

Overall this work provides clues concerning the relationships between molecular chirality induced polar order and sterically induced polar order, as well as leading to a new approach to high polarization ferroelectric LCs. Moreover, it supports the SmC$_s$P$_F$ domain model of various paraelectric and polarization randomized LC phases occurring at the cross-over between rod-like and bent molecular shapes.

4. Experimental

Synthesis

The synthesis (Scheme 1) and analytical data are reported in the ESI.† Purification was performed by column chromatography (silica gel 60, Merck, pore size 60 Å, 230–400 mesh) and/or by crystallization using the solvents described in the ESI.† ^{1}H-, and ^{13}C-NMR spectra were recorded using Varian Unity 500 and Varian Unity 400 spectrometers in CDCl$_3$ solutions using the solvent peak as an internal standard, and microanalyses were performed using a Leco CHNS-932 elemental analyzer.

Investigations

Transition temperature measurements and optical inspection of the liquid crystalline phases were performed on samples between ordinary glass slides by polarised light optical microscopy (Optiphot 2, Nikon or a Leica Leitz DMR) in conjunction with a heating stage (FP82-HT, Mettler).

Differential scanning calorimetry (Perkin-Elmer DSC-7) was performed in 30 µl-pans for 2–5 mg samples with heating and cooling rates of 10 K min^{-1}; peak temperatures for the first heating and cooling scans are given in Table 1. The assignment of the mesophases was made on the basis of the combined results of optical textures, DSC and X-ray diffraction (XRD).

XRD measurements were done at Cu-Kα line ($\mu = 1.54$ Å) using a standard Coolidge tube source with a Ni-filter. Investigations of oriented samples were performed using a 2D-detector (HI-Star, Siemens or Vantec 500, Bruker Siemens AG). Alignment was achieved by slow cooling (0.1 K min^{-1}) of a small droplet on a glass surface; the beam was applied parallel to the surface. The sample to detector distance was 8.8 cm and 26.9 cm for the wide angle and small angle measurements, respectively, and the exposure time was 30 min. Powder samples were investigated in thin capillaries ($\varnothing$ = 1 mm).

Switching experiments and electro-optical investigations were performed in a 10 µm polyimide (PI) coated ITO cell or 6 µm non-coated ITO cell (EHC, Japan) with a measuring area of 1 cm^2. The cells were filled in the isotropic state. Switching experiments were carried out with the triangular-wave method[73] using a combination of a function synthesizer (Agilent, model 33220A, load was set to 10 kΩ), an amplifier (FLC electronics, model A400), and the current response traces were recorded using an oscilloscope (Tektronix, model TDS2014) across a 5 kΩ resistance.

Acknowledgements

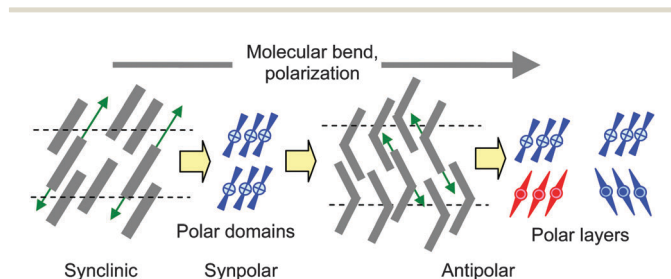**Fig. 16** Effects of out-of-plane fluctuations (green arrows) on layer coupling depending on the molecular bend.

Molecular bend, polarization

Synclinic Synpolar Antipolar Polar layers

Polar domains

References

1 (a) A. S. Tayi, A. Kaeser, M. Matsumoto, T. Aida and S. I. Stupp, *Nat. Chem.*, 2015, **7**, 281; (b) A. S. Tayi, A. K. Shveyd, A. C.-H. Sue, J. M. Szarko, B. S. Rolczynski, D. Cao, T. J. Kennedy, A. A. Sarjeant, C. L. Stern, W. F. Paxton, W. Wu, S. K. Dey, A. C. Fahrenbach, J. R. Guest, H. Mohseni, L. X. Chen, K. L. Wang, J. F. Stoddart and S. I. Stupp, *Nature*, 2012, **488**, 485.

2 R. B. Meyer, L. Liebert, L. Strzelecki and P. Keller, *J. Phys. Lett.*, 1975, **36**, L69.

3 D. Miyajima, F. Araoka, H. Takezoe, J. Kim, K. Kato, M. Takata and T. Aida, *Science*, 2012, **336**, 209.

4 (a) S. T. Lagerwall, *Ferroelectric and Antiferroelectric Liquid Cystals*, Wiley-VCH, Weinheim, 1999; (b) H.-S. Kitzerow and C. Bahr, *Chirality in Liquid Crystals*, Springer, New York, 2001.

5 R. A. Reddy and C. Tschierske, *J. Mater. Chem.*, 2006, **16**, 907.

6 G. Pelzl, S. Diele and W. Weissflog, *Adv. Mater.*, 1999, **11**(9), 707.

7 H. Takezoe and Y. Takanishi, *Jpn. J. Appl. Phys.*, 2006, **45**, 597.

8 A. Eremin and A. Jakli, *Soft Matter*, 2013, **9**, 615.

9 G. Dantlgraber, A. Eremin, S. Diele, A. Hauser, H. Kresse, G. Pelzl and C. Tschierske, *Angew. Chem., Int. Ed.*, 2002, **41**, 2408; C. Keith, R. A. Reddy, A. Hauser, U. Baumeister and C. Tschierske, *J. Am. Chem. Soc.*, 2006, **128**, 3051.

10 R. A. Reddy, C. Zhu, R. Shao, E. Körblova, T. Gong, Y. Shen, E. Garcia, M. A. Glaser, J. E. Maclennan, D. M. Walba and N. A. Clark, *Science*, 2011, **332**, 72.

11 D. R. Link, G. Natale, R. Shao, J. E. Maclennan, N. A. Clark, E. Körblova and D. M. Walba, *Science*, 1997, **278**, 1924.

12 J. P. F. Lagerwall, F. Giesselmann, M. D. Wand and D. M. Walba, *Chem. Mater.*, 2004, **16**, 3606.

13 A. Jákli, G. Liao, I. Shashikala, U. S. Hiremath and C. V. Yelamaggad, *Phys. Rev. E: Stat., Nonlinear, Soft Matter Phys.*, 2006, **74**, 041706.

14 G. Liao, I. Shashikala, C. V. Yelamaggad, D. S. Shankar Rao, S. Krishna Prasad and A. Jákli, *Phys. Rev. E: Stat., Nonlinear, Soft Matter Phys.*, 2006, **73**, 051701.

15 C. Binet, S. Rauch, C. Selbmann, P. Bault, G. Heppke, H. Sawade and A. Jakli, *Proceedings of the German Liquid Crystal Society Workshop*, Mainz, 2003, 22.

16 M. Nakata, D. R. Link, F. Araoka, J. Thisayukta, Y. Takanishi, K. Ishikawa, J. Watanabe and H. Takezoe, *Liq. Cryst.*, 2001, **28**, 1301.

17 Y. Lansac, P. K. Maiti, N. A. Clark and M. A. Glaser, *Phys. Rev. E: Stat., Nonlinear, Soft Matter Phys.*, 2003, **67**, 011703.

18 E. Gorecka, D. Pociecha, F. Araoka, D. R. Link, M. Nakata, J. Thisayukta, Y. Takanishi, K. Ishikawa, J. Watanabe and H. Takezoe, *Phys. Rev. E: Stat. Phys., Plasmas, Fluids, Relat. Interdiscip. Top.*, 2000, **62**, R4524.

19 G. Gesekus, I. Dierking, S. Gerber, M. Wulf and V. Vill, *Liq. Cryst.*, 2004, **31**, 145.

20 K. Kumazawa, M. Nakata, F. Araoka, Y. Takanishi, K. Ishikawa, J. Watanabe and H. Takezoe, *J. Mater. Chem.*, 2004, **14**, 157.

21 C. K. Lee, S. S. Kwon, T. S. Kim, E. J. Choi, S. T. Shin, W. C. Zin, D. C. Kim, J. H. Kim and L. C. Chien, *Liq. Cryst.*, 2003, **30**, 1401.

22 S. K. Lee, C. W. Park, J. G. Lee, K. T. Kang, K. Nishida, Y. Shimbo, Y. Takanishi and H. Takezoe, *Liq. Cryst.*, 2005, **32**, 1205.

23 S. K. Lee, S. Heo, J.-G. Lee, K.-T. Kang, K. Kumazawa, K. Nishida, Y. Shimbo, Y. Takanishi, J. Watanabe, T. Doi, T. Takahashi and H. Takezoe, *J. Am. Chem. Soc.*, 2005, **127**, 11085.

24 K. Nishida, M. Cepic, W. J. Kim, S. K. Lee, S. Heo, J. G. Lee, Y. Takanishi, K. Ishikawa, K.-T. Kang, J. Watanabe and H. Takezoe, *Phys. Rev. E: Stat., Nonlinear, Soft Matter Phys.*, 2006, **74**, 021704.

25 J. Thisayukta, H. Niwano, H. Takezoe and J. Watanabe, *J. Mater. Chem.*, 2001, **11**, 2717.

26 V. Novotna, K. Mieczkowska, V. Hamplova, A. Domjan, D. Pociecha, M. Kaspar and K. Fodor-Csorba, *Liq. Cryst.*, 2012, **39**, 1252.

27 S.-C. Lin, R.-M. Ho, C.-Y. Chang and C.-S. Hsu, *Chem. – Eur. J.*, 2012, **18**, 9091.

28 R. A. Reddy, B. K. Sadashiva and U. Baumeister, *J. Mater. Chem.*, 2005, **15**, 3303.

29 H. Ocak, B. Bilgin-Eran, M. Prehm, S. Schymura, J. P. F. Lagerwall and C. Tschierske, *Soft Matter*, 2011, **7**, 8266.

30 H. Ocak, B. Bilgin-Eran, D. Güzeller, M. Prehm and C. Tschierske, *Chem. Commun.*, 2015, **51**, 7512.

31 H. Ocak, B. Bilgin-Eran, M. Prehm and C. Tschierske, *Soft Matter*, 2012, **8**, 7773.

32 S. Rauch, C. Selbmann, P. Bault, H. Sawade, G. Heppke, O. Morales-Saavedra, M. Y. M. Huang and A. Jakli, *Phys. Rev. E: Stat., Nonlinear, Soft Matter Phys.*, 2004, **69**, 021707.

33 (a) G. Pelzl and W. Weissflog, in *Thermotropic Liquid Crystals: Recent Advances*, ed. A. Ramamoorthy, Springer, The Netherlands, 2007, pp. 1–58; (b) W. Weissflog, H. N. Shreenivasa Murthy, S. Diele and G. Pelzl, *Philos. Trans. R. Soc., A*, 2006, **364**, 2657.

34 (a) D. Poiecha, E. Gorecka, M. Cepic, N. Vaupotic, K. Gomola and J. Mieczkowski, *Phys. Rev. E: Stat., Nonlinear, Soft Matter Phys.*, 2005, **72**, 060701; (b) D. Poiecha, E. Gorecka, M. Cepic, N. Vaupotic and W. Weissflog, *Phys. Rev. E: Stat., Nonlinear, Soft Matter Phys.*, 2006, **74**, 021702.

35 (a) A. Eremin, H. Nadasi, G. Pelzl, S. Diele, H. Kresse, W. Weissflog and S. Grande, *Phys. Chem. Chem. Phys.*, 2004, **6**, 1290; (b) A. Eremin, M. Floegel, U. Kornek, S. Stern, R. Stannarius, H. Nadasi, W. Weissflog, C. Zhu, Y. Shen, C. S. Park, J. Maclennan and N. Clark, *Phys. Rev. E: Stat., Nonlinear, Soft Matter Phys.*, 2012, **86**, 051701.

36 M. Alaasar, M. Prehm, M. Poppe, M. Nagaraj, J. K. Vij and C. Tschierske, *Soft Matter*, 2014, **10**, 5003.

37 M. Alaasar, M. Prehm, M.-G. Tamba, N. Sebastian, A. Eremin and C. Tschierske, *ChemPhysChem*, 2016, **17**, 278.
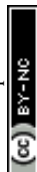
38 I. Wirth, S. Diele, A. Eremin, G. Pelzl, S. Grande, L. Kovalenko, N. Pancenko and W. Weissflog, *J. Mater. Chem.*, 2001, **11**, 1642.

39 L. Kovalenko, M. W. Schröder, R. A. Reddy, S. Diele, G. Pelzl and W. Weissflog, *Liq. Cryst.*, 2005, **32**(7), 857.

40 M. Alaasar, M. Prehm, M. Nagaraj, J. K. Vij and C. Tschierske, *Adv. Mater.*, 2013, **25**, 2186.

41 M. Alaasar, M. Prehm, K. May, A. Eremin and C. Tschierske, *Adv. Funct. Mater.*, 2014, **24**, 1703.

42 C. Keith, A. Lehmann, U. Baumeister, M. Prehm and C. Tschierske, *Soft Matter*, 2010, **6**, 1704.

43 C. Keith, M. Prehm, Y. P. Panarin, J. K. Vij and C. Tschierske, *Chem. Commun.*, 2010, **46**, 3702.

44 Y. P. Panarin, M. Nagaraj, S. Sreenilayam, J. K. Vij, A. Lehmann and C. Tschierske, *Phys. Rev. Lett.*, 2011, **107**, 247801.

45 S. P. Sreenilayam, Y. P. Panarin, J. K. Vij, V. P. Panov, A. Lehmann, M. Poppe, M. Prehm and C. Tschierske, *Nat. Commun.*, 2016, **7**, 11369, DOI: 10.1038/ncomms11369.

46 Dihydrocitronellol as a building block for rod-like ferroelectrics: J. W. Goodby, E. Chin, J. M. Geary, J. S. Patel and P. L. Finn, *J. Chem. Soc., Faraday Trans. 1*, 1987, **83**, 3429.

47 P. C. Jocelyn and N. Polgar, *J. Chem. Soc.*, 1953, 132.

48 (*a*) H. Kondo, T. Okazaki, N. Endo, S. Mihashi, A. Yamaguchi, H. Tsuruta and S. Akutagawa, *Jpn. Kokai Tokkyo Koho*, JP63033351A19880213, 1988; (*b*) E. Chin and J. W. Goodby, *Mol. Cryst. Liq. Cryst.*, 1986, **141**, 311.

49 C. V. Yelamaggad, U. S. Hiremath, S. A. Nagamani, D. S. S. Rao, S. K. Prasad, N. Iyi and T. Fujita, *Liq. Cryst.*, 2003, **30**, 681.

50 C. Tschierske and H. Zaschke, *J. Prakt. Chem.*, 1989, **331**, 365.

51 D. Güzeller, H. Ocak, B. Bilgin-Eran, M. Prehm and C. Tschierske, *J. Mater. Chem. C*, 2015, **3**, 4269.

52 (*a*) A. De Vries, *J. Chem. Phys.*, 1979, **71**, 25; (*b*) S. T. Lagerwall, P. Rudquist and F. Giesselmann, *Mol. Cryst. Liq. Cryst.*, 2009, **510**, 148; (*c*) for review, see J. P. F. Lagerwall and F. Giesselmann, *ChemPhysChem*, 2006, **7**, 20.

53 There are many disturbances in the stripe pattern, indicating weak interlayer correlations in the tilt direction.

54 The helix formation is also responsible for the smaller increase of the birefringence (pink to blue/red) on cooling the planar samples compared to *rac*-2, as the helical tilt distribution contributes to a reduction of the birefringence (Fig. 4e and f).

55 K. Gomola, L. Guo, D. Pociecha, F. Araoka, K. Ishikawa and H. Takezoe, *J. Mater. Chem.*, 2010, **20**, 7944.

56 E. Westphal, H. Gallardo, G. F. Caramori, N. Sebastian, M.-G. Tamba, A. Eremin, S. Kawauchi, M. Prehm and C. Tschierske, *Chem. – Eur. J.*, 2016, **22**, 8181.

57 In biaxial polar tilted smectic phases (and chiral tilted smectic phases) the polar direction is fixed by the tilt direction and therefore cannot be completely randomized as in the $SmAP_R$[58] and $SmAP_{AR}$[55] phases, though for the weakly bent 4-cyanoresorcinols under discussion, significant randomization of the polar direction takes place (rotation around the long axis), supported by thermal agitation.

Hence, polarization is almost randomized on a macroscopic scale with an Ising-like distribution, in the case of preferred synpolar coupling between the polarized SmC domains (SmC_sP_F domains) leading to $SmCP_R$ phases[40,41] and in the case of preferred antipolar coupling to $SmCP_{AR}$ phases.[36,37] Chirality supports synpolar coupling thus leading to a transition from $SmCP_{AR}$ to $SmCP_R^*$.

58 (*a*) Y. Shimbo, E. Gorecka, D. Pociecha, F. Araoka, M. Goto, Y. Takanishi, K. Ishikawa, J. Mieczkowski, K. Gomola and H. Takezoe, *Phys. Rev. Lett.*, 2006, **97**, 113901; (*b*) K. Gomola, L. Guo, E. Gorecka, D. Pociecha, J. Mieczkowski, K. Ishikawa and H. Takezoe, *Chem. Commun.*, 2009, 6592; (*c*) M. Gupta, S. Datta, S. Radhika, B. K. Sadashiva and A. Roy, *Soft Matter*, 2011, **7**, 4735.

59 Reducing the applied voltage also leads to a splitting into two broad separate polarization peaks, then appearing very similar to the high temperature $SmCP_{AR}$ phase (Fig. S6c–f, ESI†). This means that under reduced field strength the size of the SmC_sP_F domains is smaller.

60 M. F. Achard, J. P. Bedel, J. P. Marcerou, H. T. Nguyen and J. C. Rouillon, *Eur. Phys. J. E: Soft Matter Biol. Phys.*, 2003, **10**, 129.

61 Therefore, a prime is used to distinguish this domain type of the $SmC_s'P_A$ phase from the B_2-like SmC_sP_A phases composed of long range polar layers.

62 A similar field induced tilt in a SmA phase of an achiral molecule was reported for a hockey-stick compound: A. Eremin, S. Stern and R. Stannarius, *Phys. Rev. Lett.*, 2008, **101**, 247802.

63 There are relationships between the field-induced SmA–SmC transition and the field induced inclination in the SmC phases of compound **2** with the previously observed field induced enhancement of the clearing temperature which are all due to the presence of ferroelectric clusters: W. Weissflog, M. W. Schröder, S. Diele and G. Pelzl, *Adv. Mater.*, 2003, **15**, 630.

64 With decreasing frequency of the applied field the single peak is shifted to a lower threshold voltage, see Fig. S7 (ESI†).

65 Helix formation due to the molecular chirality might be responsible for the distinct shape of the $\beta = f(E)$ curves of (*S*)-**2** compared to *rac*-**2**.

66 L. A. Beresnev, V. G. Chigrinov, D. I. Dergachev, E. P. Poshidaev, J. Fünfschilling and M. Schadt, *Liq. Cryst.*, 1989, **5**, 1171.

67 Ferroelectric switching was previously confirmed for the chiral bent-core mesogen (*S*)-**4**, see ref. 18, though in this case no comparison with the racemate was made.

68 The field strength dependence of polarization is shown in Fig. S11 (ESI†).

69 C. Tschierske and G. Ungar, *ChemPhysChem*, 2016, **17**, 9.

70 A more detailed investigation with slowly decreasing voltage indicates that the first step of this transition is the formation of a stripe pattern during which the extinctions become parallel to the direction of the polarizers (Fig. 12f, inset) and at 0 V it turns into a smooth fan texture.

71 SmC$_s$ to SmC$_a$ transitions were also found for hockey-stick molecules, at the transition between rod-like and bent molecular shapes: E. Enz, S. Findeisen-Tandel, R. Dabrowski, F. Giesselmann, W. Weissflog, U. Baumeister and J. Lagerwall, *J. Mater. Chem.*, 2009, **19**, 2950.

72 J. Szydlowska, J. Mieczkowski, J. Matraszek, D. W. Bruce, E. Gorecka, D. Pociecha and D. Guillon, *Phys. Rev. E: Stat., Nonlinear, Soft Matter Phys.*, 2003, **67**, 031702; C. Keith, R. A. Reddy, U. Baumeister and C. Tschierske, *J. Am. Chem. Soc.*, 2004, **126**, 14312; M. W. Schröder, S. Diele, G. Pelzl and W. Weissflog, *ChemPhysChem*, 2004, **5**, 99; M. Nakata, R. F. Shao, J. E. Maclennan, W. Weissflog and N. A. Clark, *Phys. Rev. Lett.*, 2006, **96**, 067802.

73 K. Miyasato, S. Abe, H. Takezoe and A. Fukuda. E. Kuze, *Jpn. J. Appl. Phys.*, 1983, **22**, L661–L663.